

Tectonics

RESEARCH ARTICLE

10.1029/2018TC005076

Key Points:

- A belt of Upper Cretaceous (approximately 87 Ma) olistostromes, >112 km-long and 2 km in stratigraphic thickness, crops out in central Turkey
- The olistostromes contain Jurassic and Cretaceous pelagic limestone and ophiolite blocks and rest stratigraphically on a Triassic basement
- Disruption of the continental margin during a change from transform to subduction was responsible for the formation of the mass flows

Supporting Information:

- Supporting Information S1

Correspondence to:

A. I. Okay,
okay@itu.edu.tr

Citation:

Okay, A. I., Altıner, D., & Kylander-Clark, A. R. C. (2019). Major Late Cretaceous mass flows in central Turkey recording the disruption of the Mesozoic continental margin. *Tectonics*, 38, 960–989. <https://doi.org/10.1029/2018TC005076>


Received 30 MAR 2018

Accepted 12 FEB 2019

Accepted article online 21 FEB 2019

Published online 18 MAR 2019

Major Late Cretaceous Mass Flows in Central Turkey Recording the Disruption of the Mesozoic Continental Margin

Aral I. Okay¹ , Demir Altıner², and Andrew R. C. Kylander-Clark³

¹Eurasia Institute of Earth Sciences and Department of Geological Engineering, Faculty of Mines, Istanbul Technical University, Istanbul, Turkey, ²Department of Geological Engineering, Middle East Technical University, Ankara, Turkey, ³Department of Earth Sciences, University of California, Santa Barbara, California, USA

Abstract The newly recognized Upper Cretaceous (~87 Ma) olistostrome belt in central Turkey west of Ankara extends for more than 112 km subparallel to the Izmir-Ankara suture with a width of 10 km. The Alacaatlı Olistostromes are stratigraphically underlain by a Triassic basement, and are up to 2 km thick. Over 80% of the blocks in the olistostromes consist of pelagic limestones, which reach up to 300 m in size; other blocks include basalt, chert, serpentinite, tuff, and sandstone. The limestone blocks are Jurassic and Cretaceous in age with micropaleontology documenting the presence of Callovian-Oxfordian, Tithonian, Berriasian, Aptian, Albian, Cenomanian, and Turonian stages. The flows are separated by intrabasinal sediments of shale, siltstone, and volcanoclastic sandstone with Albian (108–101 Ma) detrital zircons. The olistostromes show minor tectonic deformation, and are unconformably overlain by Santonian pelagic limestones. The deposition of the Alacaatlı Olistostromes was followed by arc magmatism, which started in the Campanian (~78 Ma) after a period of shortening and uplift, and the region became a fore-arc basin with deposition of shale and volcanoclastic sandstone with Campanian (78–72 Ma) detrital zircons. A number of peculiar features of these olistostromes including rapid uplift and erosion before the creation of a deep, short-lived (89–86 Ma) ephemeral basin, dominance of deep marine limestone blocks, and inception of arc magmatism approximately 9 Myr after their deposition indicate a major tectonic event involving the disruption of the continental margin prior to the onset of arc magmatism. This event is interpreted as a change from transform margin to subduction.

1. Introduction

Olistostromes or mass transport complexes are common in the geological record, form in a variety of tectonic environments, and show a very wide variation in size and geometry (e.g., Festa et al., 2016; Moscardelli & Wood, 2016). They form through the destabilization of continental margins either through oversteepening by thrusting or folding, or through external factors such as earthquakes or tsunamis. Their age, stratigraphic position, internal composition, and geological setting provides information on the tectonic processes affecting the continental margins. Here we describe a newly recognized, very large olistostrome belt with a stratigraphic thickness of up to 2 km, which extends for more than 110 km along strike in central Turkey. To understand the origin, age, and emplacement of the Alacaatlı Olistostromes, we studied its stratigraphic position, internal structure, block types, and ages southwest and north of Ankara, and established for the first time its wide extent in the central Anatolia, and put forward a model for its origin. The deposition of the olistostromes signifies a major tectonic event involving the whole-scale disruption of the continental margin prior to the onset of arc magmatism. Using constraints from biostratigraphy, geochronology, and geology, we show that this event is probably related to a change from transform margin to subduction.

2. Tectonic Setting and Stratigraphy of the Ankara Region

The olistostrome belt is located in the Pontides, which constituted part of the Mesozoic continental margin of Eurasia (Okay & Nikishin, 2015). The Pontides consist of three terranes: the Sakarya and Istanbul zones and the Strandja Massif (Okay & Tüysüz, 1999). The basement of the Sakarya Zone is mostly made up of Triassic subduction-accretion complexes of deformed turbidites and basalts, called the Karakaya Complex. The Karakaya Complex is unconformably overlain by a 2-km-thick Jurassic-Cretaceous

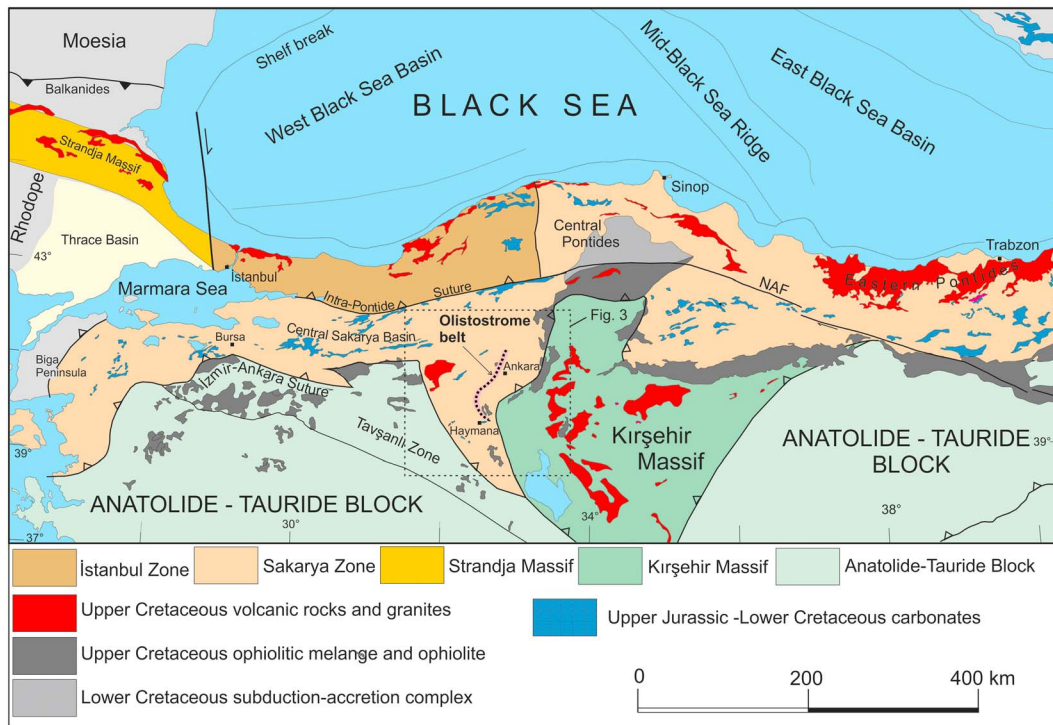


Figure 1. Tectonic map of the Circum-Black Sea region showing the location of the Late Cretaceous olistostromal belt. Modified from Okay and Altıner (2016).

sedimentary and volcanic sequence, which is well exposed in the central Sakarya Basin in northwest Turkey (Figure 2; Altıner et al., 1991; Ocakoğlu et al., 2018).

In the central Pontides, the Istanbul and Sakarya zones were amalgamated before the Late Jurassic, as shown by a common Upper Jurassic–Lower Cretaceous carbonate cover (Figure 1; Okay et al., 2018), whereas an oceanic embayment continued to exist between these zones in northwest Turkey along the present North Anatolian Fault (Figure 1). This oceanic embayment is represented by the Intra-Pontide suture (Şengör & Yılmaz, 1981), which is marked by Cretaceous ophiolitic mélanges and metamorphic rocks (Akbaş et al., 2013); in the east it joins to the large Cretaceous subduction–accretion complexes of the central Pontides (Figure 1).

The Sakarya Zone is bordered in the south by the Anatolide-Tauride Block and the Kırşehir Massif along the İzmir-Ankara suture (Figure 1). The İzmir-Ankara suture represents the major Tethyan ocean with documented episodes of northward subduction during the Late Triassic (210–200 Ma), Jurassic (172–158 Ma), Early Cretaceous (110–100 Ma), and Late Cretaceous (e.g., Okay & Nikishin, 2015). The Black Sea opened as an oceanic back-arc basin during the Santonian, and led to the separation of the Pontides from Eurasia (e.g., Nikishin et al., 2015). The episodes of documented subduction were separated by periods of quiescence; most notably in the Late Jurassic–Early Cretaceous (157–130 Ma) when carbonates were deposited throughout the Black Sea region with no evidence of active subduction (e.g., Vincent et al., 2018). Oceanic subduction under the Pontides ended in the latest Cretaceous to Paleocene when the Pontides collided with the Anatolide-Tauride Block leading to the north-vergent deformation of the Pontide margin.

The Anatolide-Tauride Block shows a similar stratigraphy to the Arabian Plate, from which it was separated during the Permo-Triassic with the creation of the Eastern Mediterranean-Bitlis Ocean (Şengör & Yılmaz, 1981). The northwestern promontory of the Anatolide-Tauride Block was subducted in the Late Cretaceous in an intraoceanic subduction zone, leading to ophiolite obduction, HP-LT metamorphism, and deformation of the continental margin at 90–80 Ma as seen in the Tavşanlı Zone in northwest Turkey (Figure 1; Okay & Whitney, 2010).

The Kırşehir Massif, located between the Pontides and the Anatolide-Tauride Block, consists of high-grade metamorphic rocks with Late Cretaceous metamorphic ages (91–83 Ma) and dismembered ophiolites

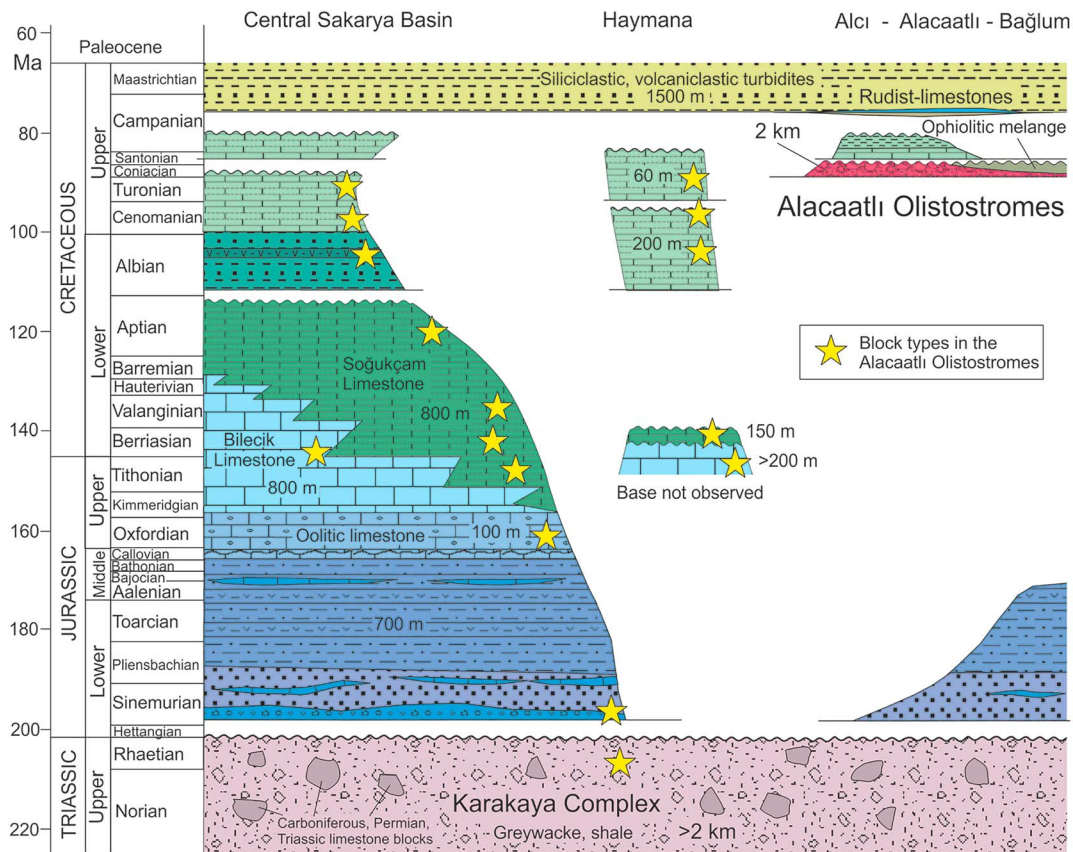


Figure 2. Generalized stratigraphic section of the Ankara region and the central Sakarya Basin. The yellow stars indicate the block types found in the Alacaatlı Olistostromes.

intruded by Late Cretaceous granites (85–70 Ma; Figure 2; e.g., Whitney & Hamilton, 2004; van Hinsbergen et al., 2016). It was a continental platform, with affinities to the Anatolide-Tauride Block, which underwent metamorphism under an obducted Cretaceous ophiolite followed by the construction of a magmatic arc during the Late Cretaceous; the collision of this Kırşehir arc with the Pontides occurred in the late Maastrichtian-Paleocene and produced the arc-shaped geometry of the central Pontides (Figure 1; Meijers et al., 2010) and the present-day triangular shape of the Kırşehir Massif, which is a result of folding of the originally north-south trending Kırşehir magmatic arc (Lefebvre et al., 2013).

The Ankara region lies in the Sakarya Zone close to the İzmir-Ankara suture (Figure 1). The area is well known for mélanges since the early work of Bailey and McCallien (1950) and Bailey and McCallien (1953). Subsequent work showed that the mélanges around Ankara are of different types and ages (Batman, 1978; Boccaletti et al., 1966; Koçyiğit, 1991; Ünal, 1981). The most widespread is the Karakaya Complex with exotic blocks of Carboniferous, Permian, and Triassic limestone in a strongly sheared greywacke-shale matrix, which also constitutes the lowest stratigraphic unit in the Ankara region. The Karakaya Complex is now regarded as Triassic trench sediments of the Paleo-Tethys (e.g., Okay & Göncüoğlu, 2004). It crops out along a 20-km-wide and 180-km-long belt east of Ankara (Figure 3), where it is unconformably overlain in a few places by a Lower-Middle Jurassic fluviatile to shallow marine clastic sequence with horizons of red nodular limestone, which have yielded Lower and Middle Jurassic ammonites (Alkaya & Meister, 1995; Bremer, 1966; Deli & Orhan, 2007; Koçyiğit, 1987; Kuznetsova et al., 2003; Varol & Gökten, 1994). Higher in the stratigraphic sequence are Upper Jurassic–Lower Cretaceous shallow marine carbonates, which crop out in the Haymana area west of Ankara (Figure 3); these are unconformably overlain by deep marine Cretaceous limestone sequences (Figure 2, Okay & Altın, 2016).

The second type of mélange in the Ankara region is the ophiolitic mélange, which mainly crops out in a 15–20-km-wide belt east of the Karakaya Complex and extends for more than 250 km from Çankırı to the

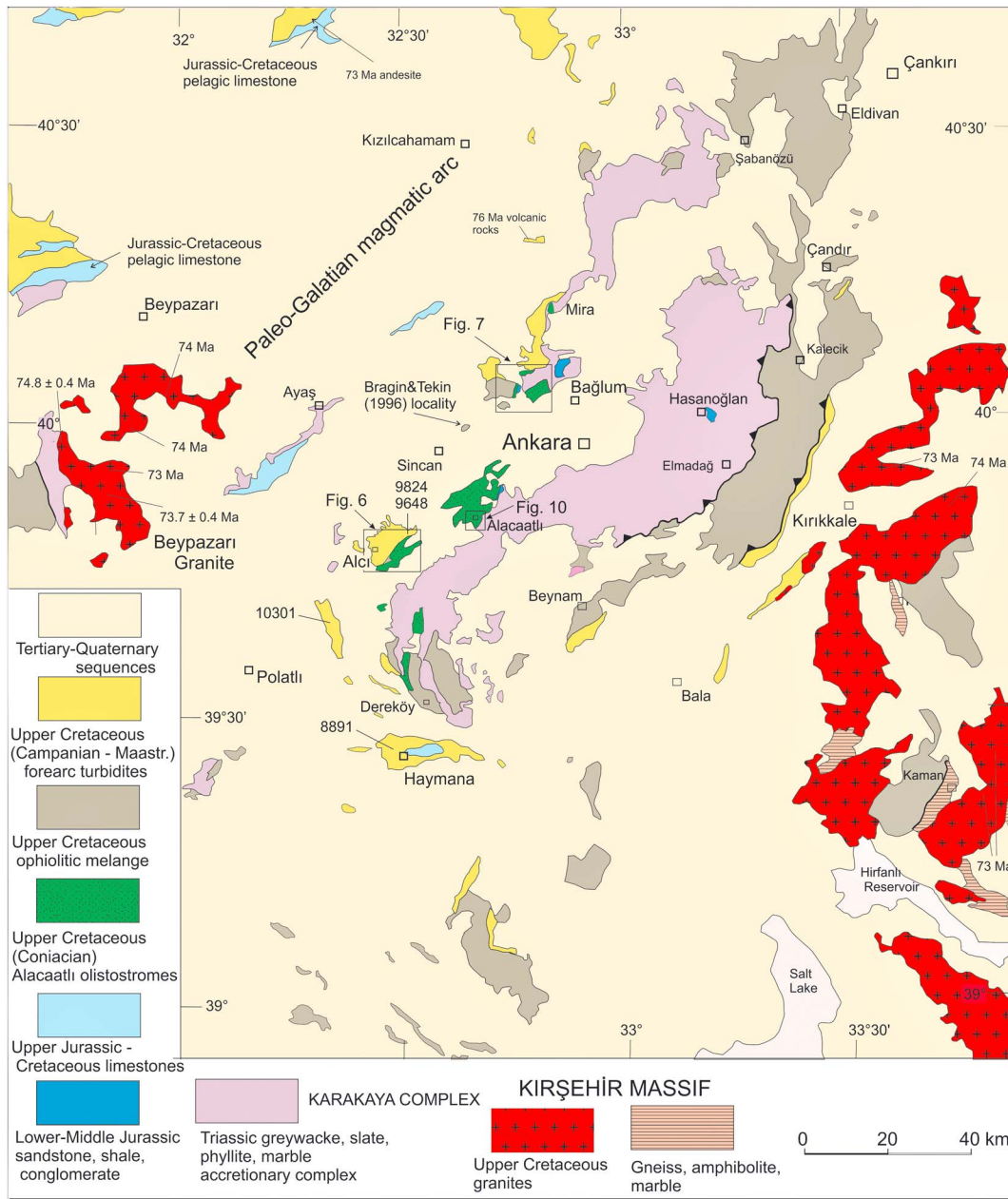


Figure 3. Geological map of the Ankara region modified from Turhan (2002). The isotopic ages, mostly zircon U-Pb, are from Keller et al. (1992), Koçyiğit et al. (2003), Köksal et al. (2004), Delibaş et al. (2011), and Helvacı et al. (2014).

Salt Lake (Figure 3). The ophiolitic mélangé consists of basalt, radiolarian chert, serpentinite, and limestone, with lesser amounts of gabbro, diabase, shale, and sandstone (Çapan & Buket, 1975; Dangerfield et al., 2011; Rojay, 2013; Sarifakioğlu et al., 2014; Tankut et al., 1998). It includes semiintact ophiolite bodies (Üner et al., 2014; Uysal et al., 2016) with Jurassic ages (Çelik et al., 2013; Dilek & Thy, 2006). The cherts in the ophiolitic mélangés have yielded Triassic, Jurassic, and Lower Cretaceous radiolarian ages (Sarifakioğlu et al., 2014; Bortolotti et al., 2018), and some of the pelagic limestones associated with pillow lavas are Lower Cretaceous (Barremian; Rojay et al., 2004). The presence of Lower Cretaceous (Barremian) cherts and limestones suggests that the ophiolitic mélangé represents an Upper Cretaceous accretion complex resulting from the subduction of a Mesozoic Tethyan ocean. The contact between the Karakaya Complex and the ophiolitic mélangé defines the İzmir-Ankara Suture between the Pontides and the Kırşehir Massif (Figures 1 and 3).

The third type of blocky unit, which forms the subject of this study, consists of Jurassic and Cretaceous limestone and locally ophiolitic blocks in a largely undeformed silty-marly matrix. It crops out along an up to 10-km-wide and 112-km-long zone west of the Karakaya belt (Figure 3). It was first described as a distinct Cretaceous stratigraphic and sedimentary unit in the Alacaatlı region southwest of Ankara by Batman et al. (1978), who mapped the olistostromes as the Alacaatlı mélange. Ünal (1981) recognized the olistostromes from the Bağlum region north of Ankara as the “unit with limestone blocks.” Koçyiğit (1991), Deli and Orhan (2007), and Rojay (2013) described the olistostromes as a “sedimentary mélange.”

3. Methods

We used geological mapping, micropaleontology, and geochronology to constrain the stratigraphic position of the olistostromes, the source of the blocks, the age of the intrabasinal sediments, and the inception of arc magmatism in the Ankara region. The geological mapping was carried out on 1:25,000 scale topographic maps. The UTM grid on the European 1979 datum is used in the maps and in the location of the outcrops and the samples. Over 250 samples collected during mapping were studied in thin section for micropaleontology to find the age of the blocks and to constrain their source. Information on the size, age, and locality of the blocks are given in Table S3; the sample numbers in the table are linked to those in the geological maps in Figures 6, 7, and 9. Benthic and planktonic foraminifera and calpionellids, which are important for dating, have been identified based on Altner (1991), Altner and Özkan (1991), and Premoli Silva and Verga (2004). Photomicrographs of identified Mesozoic foraminifera and calpionellids are given in Figures S1, S2, and S3.

For geochronology we used zircon U–Pb and biotite Ar–Ar techniques. Zircon and biotite were separated from rock samples in Istanbul Technical University using standard mineral separation procedures. The zircons were picked under a stereographic microscope and mounted in epoxy and were polished and analyzed using laser ablation–inductively coupled plasma mass spectrometry (LA-ICPMS) at the University of California, Santa Barbara (Kylander-Clark et al., 2013). For the details of the method employed, see Okay et al. (2014). Long-term reproducibility in secondary reference materials is <2%, and as such, should be used when comparing ages obtained within this analytical session, to ages elsewhere. Biotites were dated using the Ar–Ar single-grain fusion method at the Open University in the UK. For the details of the method see Okay et al. (2014). The U–Pb and Ar–Ar analytical data are given in Tables S1 and S2, respectively.

4. Alacaatlı Olistostromes: Mass Flows With Pelagic Limestone Blocks

The Alacaatlı Olistostromes consist of very poorly sorted, chaotic breccias with angular, subangular, rounded blocks in a silty, marly matrix (Figures 4 and 5). Over 90% of the blocks are pelagic limestone; the rest consist of green tuff, red radiolarian chert, Jurassic shallow marine limestone, greywacke, shale, and siltstone (Figure 5). Ophiolitic blocks are restricted to certain regions and are generally not mixed with limestone blocks. The size of the clasts ranges from millimeters to several hundred meters, and is principally controlled by the mechanical strength of the blocks. The 100-m-sized blocks are generally made up of strongly lithified clay-free limestones of Callovian-Oxfordian or Tithonian-Berriasian ages; they tend to be concentrated in the lower stratigraphic levels of the olistostromal sequence. Disregarding the large blocks, the clast size in the olistostromes in a typical outcrop ranges from millimeters to tens of meters with most of the clasts in the range of 5 to 25 cm (Figures 5a and 5b). Olgun and Norman (1993) made a study of the clast size and shape of the outcrop-scale olistostromes using photo-grid method. They found that the average block size in an outcrop ranges between 6 and 50 cm, the sorting is very poor, and the clasts are angular to subangular. The clasts are predominantly matrix-supported; the matrix to block ratio is 20:80 and the matrix commonly shows no penetrative deformation. The blocks generally do not show any preferred orientation (Olgun & Norman, 1993); their shape is generally tabular or equant (Figures 5a and 5b). The thickness of individual olistostromal horizons ranges from ten meters to over 50 m. Individual olistostromal flows are difficult to distinguish in outcrop unless separated by intrabasinal sediments (Figure 4a), which consist of mudstone, siltstone, and sandstone; some of the thicker intrabasinal horizons are shown in the geological map in Figure 6. The lateral continuity of the intrabasinal sediments are commonly disrupted by the arrival of the younger mass flows.

There is no cleavage or lineation in the matrix of the olistostromes; the contacts between the blocks and the matrix are sedimentary (Figure 5). The only deformation observed is rare drag folds and shear zones likely

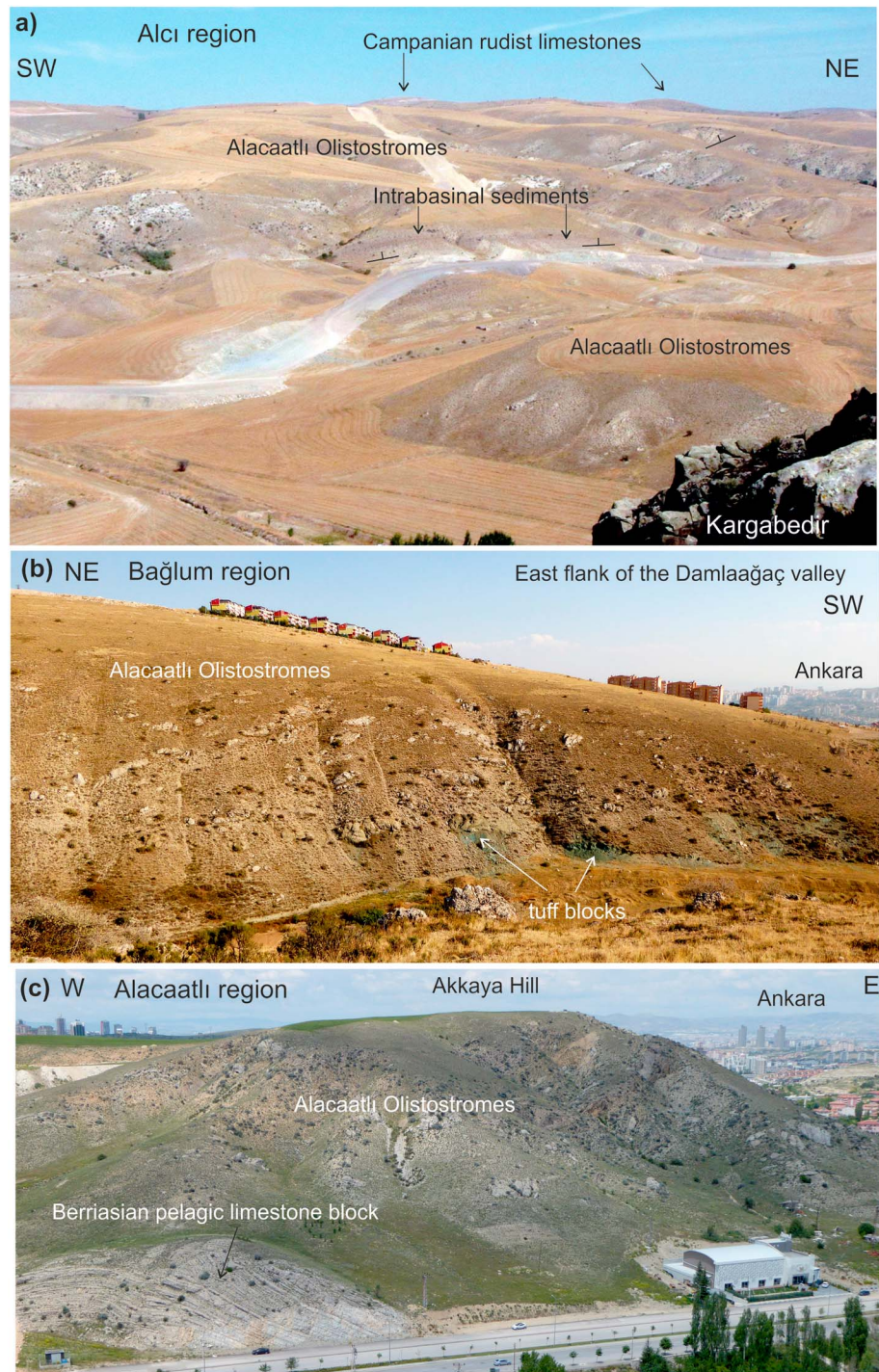


Figure 4. General overview of the Alacaatlı Olistostromes in the (a) Alcı, (b) Bağlum, and (c) Alacaatlı regions. (a) The field of view up to the Campanian rudist-limestones in the horizon is made up of olistostromes (cf. Figure 6). (b) The limestone blocks in the photograph define a low-angle bedding dipping to the east (left). Note the green tuff blocks in the basal part of the sequence. (c) Olistostromes with a 150-m-large block of Berriasian pelagic limestone (cf. Figure 10).

induced during sliding into the basin. Postdepositional penetrative deformation and compaction of the olistostromes are insignificant.

We studied the olistostromes in the Alcı and Alacaatlı areas southwest of Ankara and Bağlum and Mira regions north of Ankara (Figure 2). In the Alcı area the olistostromes crop out over an area of 10 km by

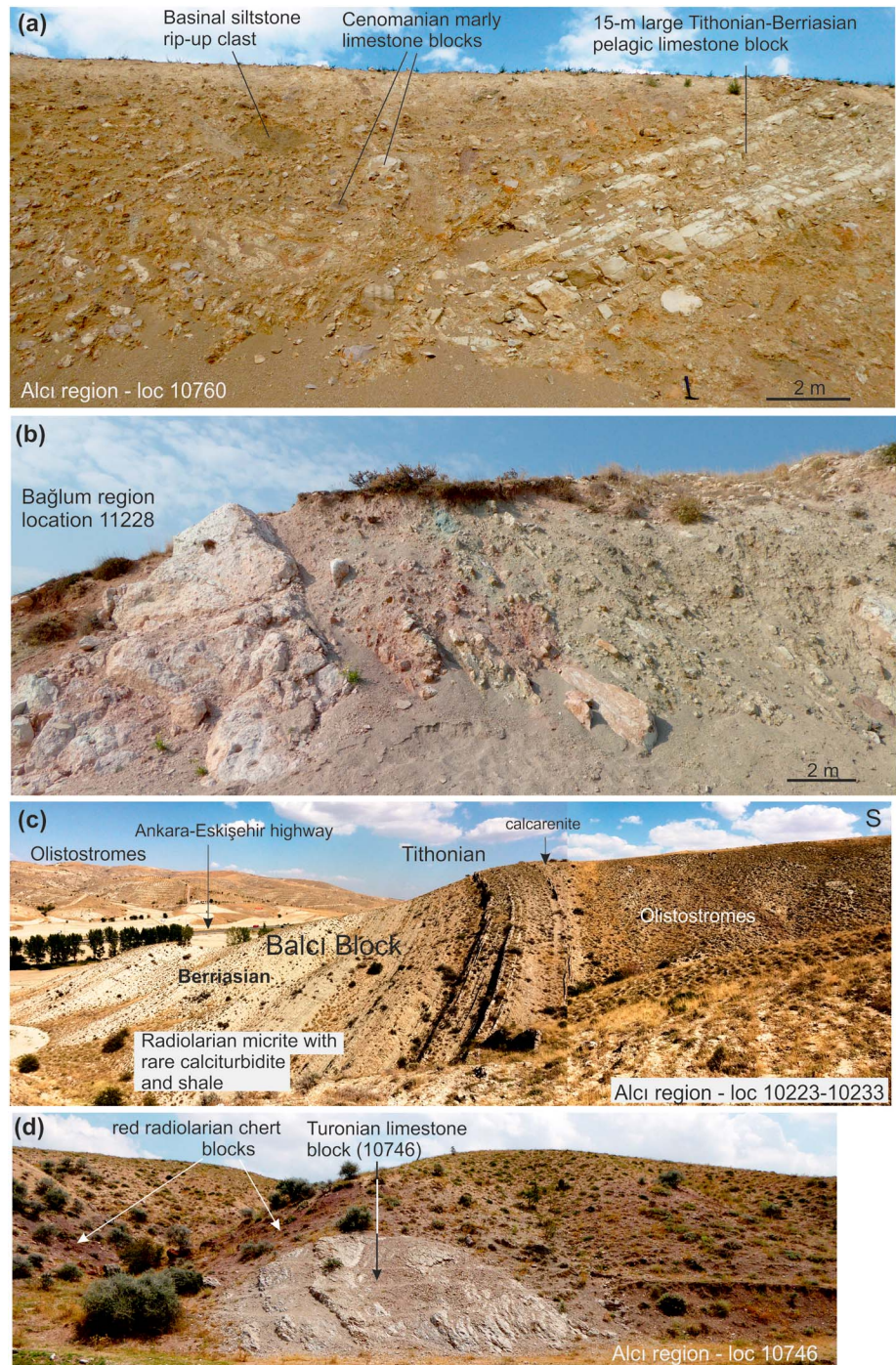


Figure 5. Field photographs of the Alacaatlı Olistostromes. Typical view of the olistostromes in the (a) Alcı and (b) Bağlum regions. Note the poor sorting and lack of penetrative deformation. (c) The 200-m-thick Upper Jurassic–Lower Cretaceous pelagic limestone block in the Alcı region. The well-exposed block is surrounded by olistostromes with smaller limestone blocks (cf. Figure 6). (d) Turonian block of pelagic marly limestone and shale surrounded by the radiolarian chert blocks.

5 km and dip at moderate angles under the Campanian rudist-limestones, which indicates a stratigraphic thickness of ~2 km (Figures 4a and 6). In the Bağlum area, the Alacaatlı Olistostromes form isolated outcrops due to later tectonics and have a preserved stratigraphic thickness of about 700 m (Figure 7).

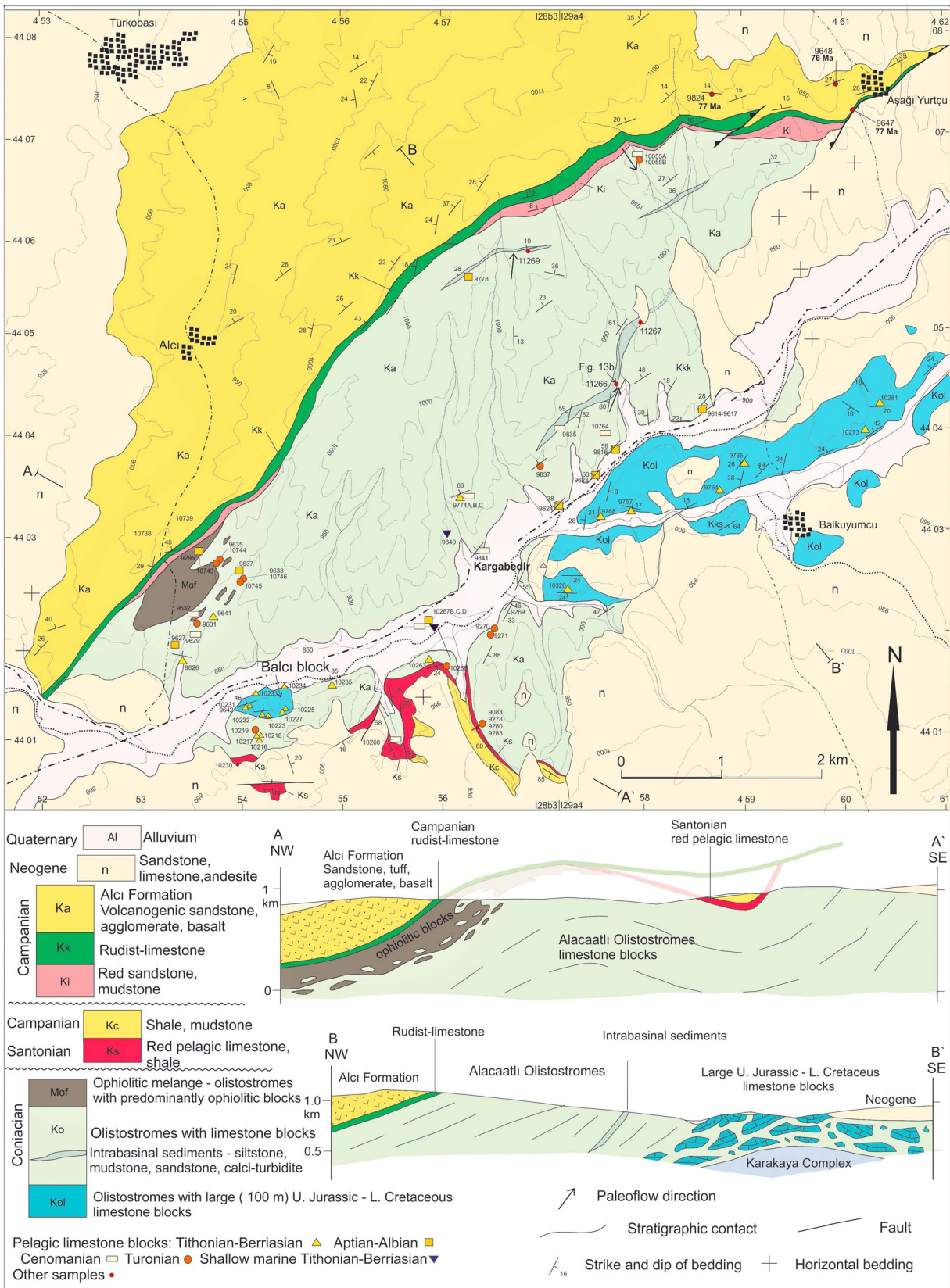


Figure 6. Geological map and cross section of the Alci region. For location see Figure 3. The map is based on our mapping and on Rojay and Süzen (1997).

4.1. Stratigraphic Base

The base of the Alacaatlı Olistostromes is well exposed in the Bağlum region, where the olistostromes lie stratigraphically with a subhorizontal contact over the Karakaya Complex or over the Lower Jurassic sandstones (Figures 7 and 8). The Karakaya Complex in the Bağlum region consists of highly deformed greywacke, siltstone, and shale. In the north, close to the Radar Tepe (Figure 7), the greywackes contain shallow marine limestone blocks, several tens of meters across. The limestones contain Middle Triassic (Anisian-Ladinian) foraminifera *Trochamina almtalensis* and *Endotriadella wirzi*, which confirm the Late Triassic age of the Karakaya complex.

North of the Yakacık village in the Bağlum area, the olistostromes lie stratigraphically over a Lower Jurassic sequence of calcareous sandstone, siltstone, and conglomerate with red limestone horizons, which itself lies unconformably over the Karakaya Complex (Figure 7; Ünal, 1981). The Jurassic sequence has a rich ammonite and brachiopod fauna of Sinemurian-Pliensbachian age (Ager, 1959; Vörös, 2014), and we have also determined *Involutina liassica* and *Agerina martana* in the calcareous sandstone (14 in Figure S1), which confirms the Early Jurassic age.

4.2. Sedimentary Blocks and Ages

4.2.1. Upper Triassic Greywacke

In the Bağlum area there are lenses of breccia and pebbly sandstone at the basal levels of the olistostromes (Figure 7). This clastic sequence is up to 50 m thick and consists of very poorly sorted, angular greywacke clasts, 1 to 40 cm across, in an undeformed silty sandy matrix. Apart from the dominant greywacke clasts, derived from the underlying Karakaya Complex, there are also rare clasts of well-rounded granite, common in the Lower Jurassic conglomerates, and pelagic limestone, the latter may reach 5 m in size. One such large limestone block (11230A) contains an early Berriasian fauna of *Calpionella alpina* (spherical forms) and *Tintinopsella carpathica*. Another smaller limestone block (11230C) is of Middle-Upper Jurassic (Callovian-Oxfordian) age based on the abundance of *Globuligerina* gr. *oxfordiana*. The presence of the Cretaceous and Middle-Upper Jurassic limestone clasts shows that this clastic sequence, previously mapped as Lower Jurassic, represents the basal part of the Alacaatlı Olistostromes.

4.2.2. Middle-Upper Jurassic Oolitic Limestone

These blocks are made up of massive, white to light gray, and commonly oolitic limestones, which are commonly larger than 40 m across; they are found in the Bağlum, Alacaatlı, and Mira areas (Table S3). Fourteen samples from these blocks yielded a Callovian-Oxfordian foraminifera fauna including *Globuligerina* gr. *oxfordiana*, *Palaeomiliolina strumosum*, *Globochaete alpina*, and *Reophax* sp. (12, 14–17, 22–23 in Figure S1). Autochthonous limestone sequences of similar facies and age are known from the western Sakarya Zone, where they lie stratigraphically above the Lower Jurassic clastic rocks and form the basal part of the Bilecik Group carbonates (Altner, 1991).

4.2.3. Uppermost Jurassic–Lower Cretaceous Pelagic Limestone and Calciturbidite

By volume and number the uppermost Jurassic–Lower Cretaceous pelagic limestone form the largest population of blocks in the Alacaatlı Olistostromes with blocks ranging from a few millimeters to several hundred meters in size (Rojay & Sözen, 1997). They also form the largest blocks in the Alçı and Alacaatlı regions.

Uppermost Jurassic–Lower Cretaceous blocks consist of thinly to medium-bedded white, light gray radiolaria-bearing micritic limestone with gray chert nodules, and minor shale and calciturbidite beds. Overall 75% of the sequence consists of radiolarian biomicrite, 17% of calciturbidite, and 7% of gray chert nodules and lenses. The large blocks preserve their internal stratigraphy. One such block, which is well exposed south of Alçı has a stratigraphic thickness of 200 m (Figures 5c and 6). Stratigraphically the basal parts of this block, named as the Balçı block, consists of radiolarian biomicrites intercalated with calciturbidite beds and laminated turbiditic calcareous sandstones. Four samples from this part contain *Saccocoma* sp., *Belorussiella* sp., and *Globochaete alpina* (20, 21, 12 in Figure S1). This assemblage corresponds to the Tithonian *Saccocoma* zone of Altner (1991). The bulk of the Balçı block consists of thin- to medium-bedded radiolarian biomicrites intercalated with marly limestone (Figure 5c). Samples from this part contain Tithonian–lower Berriasian foraminifera and calpionellids including *Calpionella alpina*, *Crassicollaria masutiniana*, *C. parvula*, *Crassicollaria* sp., and *Spirillina* sp. (24–30, 46–50 in Figure S1). The fauna corresponds to the upper Tithonian A and lower Berriasian B calpionellid zones described by Altner and Özkan (1991) from the central Sakarya Basin. A sample taken from the topmost part of the Alçı Block

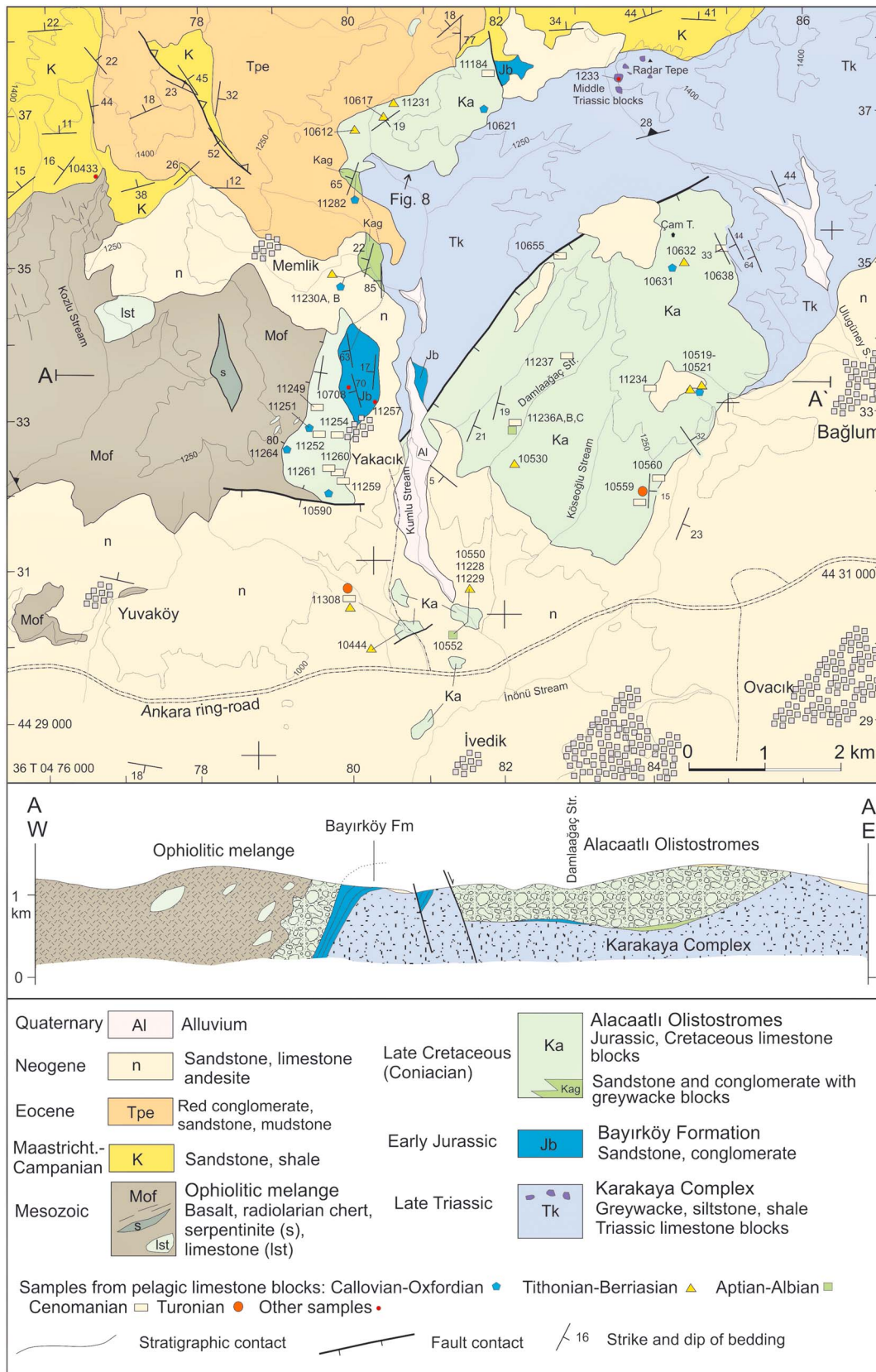


Figure 7. Geological map and cross section of the Bağlum region. For location see Figure 2.

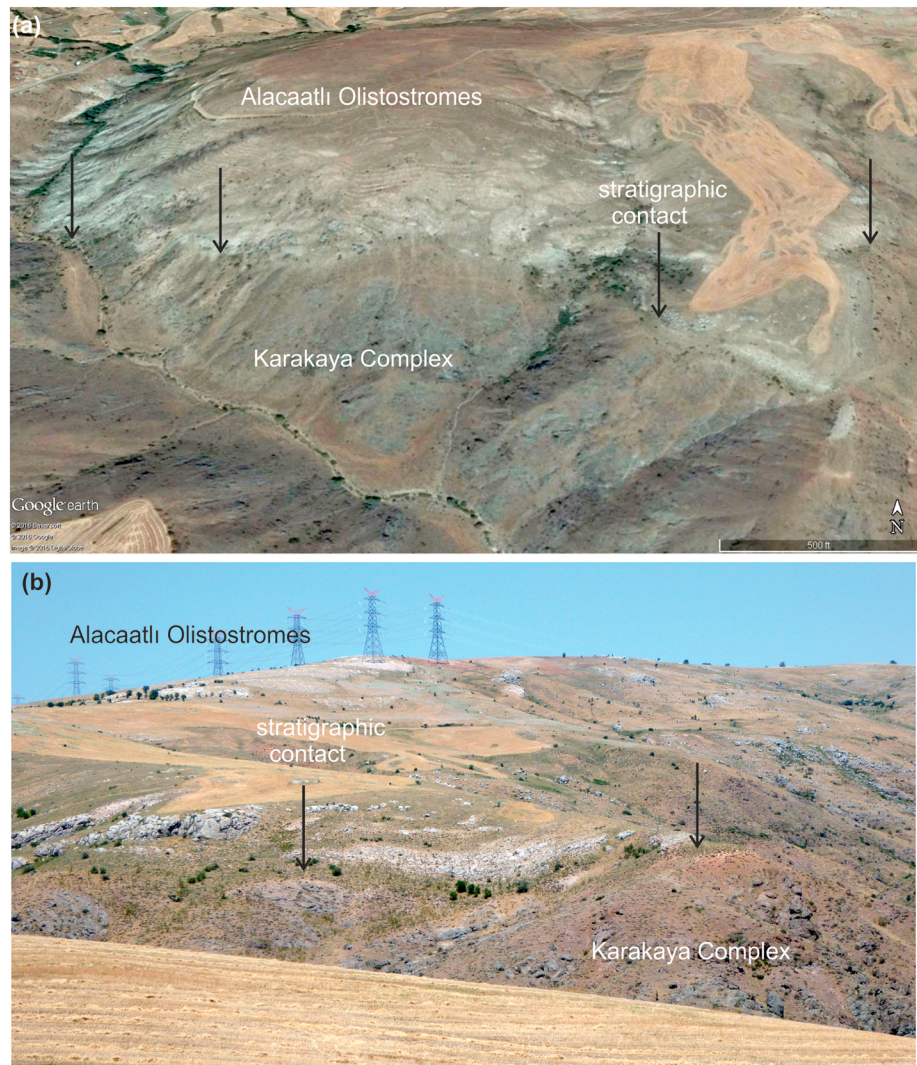


Figure 8. The subhorizontal stratigraphic contact between the Alacaatlı Olistostromes and the underlying Upper Triassic greywackes of the Karakaya Complex in Google Earth image and in the field. The arrows point the contact.

(sample 10234) contains a middle Berriasian (calpionellid C zone) fauna of *Calpionella alpina* and *Calpionella elliptica* (24–30, 33–35 in Figure S1). Thus, the 200-m-thick Balcı Block is of Tithonian-Berriasian age and preserves the Jurassic–Cretaceous transition.

Over 40 blocks of uppermost Jurassic–Lower Cretaceous pelagic limestone and calciturbidites were sampled in the Alcı, Bağlum, and Alacaatlı areas (Table S3). Tithonian blocks are generally rare and are characterized by the abundance of radiolaria and the pelagic crinoid *Saccocoma*. Most of the blocks are early Berriasian in age (Calpionellid B zone) with *Calpionella alpina* (spherical forms), *Crassicollaria parvula*, *C. brevis*, and *Remaniella ferasini* with some middle Berriasian (Calpionellid C zone) with *Calpionella alpina*, *C. elliptica*, *Tintinopsella carpathica*, and *Crassicollaria parvula* and upper Berriasian (Calpionellid D zone) with *Calpionellopsis oblonga*, *Calpionellopsis simplex*, *Tintinopsella carpathica*, *T. longa*, and *Remaniella cadischiana* limestone blocks (24–30, 36–45, 49–50 in Figure S1 and Table S3). Many of the pelagic limestone blocks in the Alcı area contain only radiolaria, which in some of these blocks are dated to the late Valanginian (Mekik, 2000).

The calciturbidite beds in the Tithonian-Berriasian limestone blocks measure from a few centimeters to a few meters in thickness; they show graded bedding and flute casts and consists predominantly of transported shallow marine limestone clasts; and the clasts contain Kimmeridgian-Berriasian benthic foraminifera and

The uppermost Jurassic–Lower Cretaceous pelagic limestone sequence from which the blocks were derived must have been at least 200 m thick. Altuner and Özkan (1991) and Mekik et al. (1999) have measured thicknesses of 400 to 770 m in the autochthonous uppermost Jurassic–Lower Cretaceous (Tithonian–Berriasian) pelagic limestone sequences in the central Sakarya Basin (Figure 3), and Tunç (1993) described 285 m of Tithonian–Valanginian pelagic biomicrites overlying Kimmeridgian shallow marine limestones northwest of Kızılcahamam (Figure 2).

4.2.4. Upper Jurassic–Lower Cretaceous Shallow Marine Limestone

In the central Sakarya Basin and in the Haymana area the Upper Jurassic–Lower Cretaceous shallow marine carbonates, ascribed to the Bilecik Group, form sequences over 600 m thick (Figure 2; Altunlu, 1976; Altuner, 1991; Altuner et al., 1991; Okay & Altuner, 2016). However, such limestones make up less than 2% of the blocks in the Alacaatlı Olistostromes; they are generally less than a few meters in size and consist of grainstones with abundant algae and intraclasts. The benthic foraminifera in two sampled blocks in the Alcı area include *Protopenneroplis ultragranulata*, *Crescentiella morronensis*, *Crescentiella* sp., *Charentia* sp., and *Neotrocholina* sp. (3–4, 6, 8–11 in Figure S1 and Table S3) and indicate a middle Tithonian–Berriasian age range. They are more common as clasts in the calciturbidites in the uppermost Jurassic–Lower Cretaceous pelagic limestone blocks.

4.2.5. Lower Cretaceous Marly Limestone, Calciturbidite, and Breccia

Aptian blocks are rare but occur in the Alcı, Bağlum, and Alacaatlı areas; they consist of gray, pink marly limestone. A 10-m-large marly limestone block (sample 9637), associated with ophiolitic blocks south of Alcı, contains a Late Aptian fauna of *Globigerinelloides ferreolensis*, *Hedbergella infracretacea*, *Hedbergella* sp., and *Globigerinelloides* sp. (51–54, 63–68, 73, and 77–90 in Figure S1). Another smaller limestone block from the same region also contains late Aptian foraminifera of *Globigerinelloides algerianus*, *Hedbergella trochoidea*, and *Hedbergella* sp. (55–57 and 69–72 in Figure S1).

A variety of deep marine facies ranging from radiolarian biomicrite, marly limestone, marl, calciturbidite, and breccia are found in the Albian blocks, which are recorded in the Alcı, Alacaatlı, and Bağlum areas. More than 10 Albian blocks have been paleontologically determined in the Alcı area (Table S3). An 8-m-large block consists of calciturbidite and breccia. A sample from the calciturbidite horizon (9615) contains Albian foraminifera *Ticinella roberti* and *Muricohedbergella planispira* (74–76 and 80–81 in Figure S1) as well as clasts of the Bilecik Limestone with *Protopenneroplis ultragranulata*, *Coscinoconus delphinensis*, and *Mohlerina basiliensis* (3–5, 13 in Figure S1). The Albian foraminiferal fauna in the other Albian blocks includes *Ticinella roberti*, *T. praeticinensis*, *T. raynaudi*, *Ticinella* sp., *Muricohedbergella delrioensis*, *M. planispira*, *M. rischi*, *Macroglobigerinelloides ultramicrus*, and *Lenticulina* sp. (74–83 in Figure S1).

Autochthonous Albian sequences are known from the Haymana region and from the central Sakarya Basin (Figure 3; Okay & Altuner, 2016). In the Haymana region the Albian–Cenomanian sequence consists of marl, marly limestone, calciturbidite, breccia, and sandstone, which rests unconformably over the Bilecik and Soğukçam limestones. In the central Sakarya Basin Albian is represented by volcanogenic sandstone and limestone (Figure 3; Yilmaz, 2008).

4.2.6. Cenomanian Marly Limestone, Radiolarian Biomicrite

The Cenomanian blocks in the Alacaatlı Olistostromes are made up of gray, greenish gray, pink marly limestone and marl. In contrast to the Albian blocks there are no calciturbidite and breccia beds in the Cenomanian blocks. Cenomanian blocks are generally 10 to 40 cm across, smaller than the Lower Cretaceous blocks; however, rare 20-m-large Cenomanian blocks are recorded in the Alcı area. Cenomanian blocks are found in the Alcı, Bağlum, and Alacaatlı areas. Foraminiferal fauna from nine Cenomanian limestone blocks in the Alcı area and two from the Bağlum area (Table S3) include *Rotalipora cushmani*, *Rotalipora* sp., *Thalmaninella deecki*, *T. greenhornensis*, *T. reicheli*, *T. globotruncanoides*, *T. appenninica*, *T. balernaensis*, *Praeglobotruncana stephani*, *P. delrioensis*, *Heterohelix moremani*, *Whiteinella praehelvetica*, *Whiteinella* sp., *Muricohedbergella planispira*, *M. delrioensis*, and *Macroglobigerinelloides* sp. (84 in Figure S1; 1–12, 21–23, 37, and 41–42 in Figure S2; and Table S3).

4.2.7. Turonian Marly Limestone, Radiolarian Biomicrite

Turonian limestone blocks are widely distributed in the Alcı area with a preferred occurrence near the ophiolitic blocks (Figure 6); they are also found in the Alacaatlı and Bağlum regions (Figures 7 and 9). They constitute the youngest blocks in the Alacaatlı Olistostromes. The Turonian blocks consist of light gray, cream, light pink marly limestone with a rich fauna of planktonic foraminifera. Turonian foraminifera have

been found in 13 sampled blocks in the Alcı area (Table S3); the block size ranges from a few tens of centimeters up to 20 m (Figure 5d). Three samples from a 10-m-long marly limestone block in the Alcı area (9638, 10746) contain *Marginotruncana pseudolinneiana*, *M. coronata*, *M. renzi*, *M. marginata*, *Dicarinella primitiva*, *Whiteinella paradubia*, *Whiteinella aprica* or *baltica*, *Whiteinella* spp., *Muricohedbergella flandrini*, *M. planispira*, and *Heterohelix globulosa* (26–32, 47–49, 53, and 56–58 in Figure S2 and 9–14, 21–22 in Figure S3). The presence of *Dicarinella primitiva* (age range latest Turonian–Coniacian) together with *Whiteinella paradubia* (late Cenomanian–middle Coniacian) indicates a latest Turonian to middle Coniacian age (approximately 90–88 Ma) for this block. Another marly limestone block (9635) contains *Marginotruncana pseudolinneiana*, *Marginotruncana* sp., *Dicarinella primitiva*, *D. algeriana*, and *Heterohelix moremani* (50–51 and 54–58 in Figure S2 and 13–14 in Figure S3). The presence of *Dicarinella primitiva* (age range latest Turonian–Coniacian) together with *Whiteinella paradubia* (latest Cenomanian–Turonian) indicates a latest Turonian age for the block. A pinkish gray marly limestone block (sample 11435), 1.5 m across, from the Alacaatlı area also yielded a similar late Turonian fauna of *Marginotruncana pseudolinneiana*, *M. coronata*, *M. renzi*, *Dicarinella primitiva*, and *Helvetoglobotruncana helvetica*.

Lower-Middle Turonian blocks are common in the vicinity of the ophiolitic blocks. Nine such marly limestone blocks, ranging from 2 to 20 m across, were sampled. The foraminifera in the blocks include *Helvetoglobotruncana helvetica*, *Marginotruncana renzi*, *M. pseudolinneiana*, *M. cf. sinuosa*, *M. schneegansi*, *M. sigali*, *Whiteinella prae-helvetica*, *W. archaeocretacea*, *Whiteinella* sp., *Dicarinella canaliculata*, *Heterohelix globulosa*, *H. moremani*, *Muricohedbergella planispira*, *M. delrioensis*, *Muricohedbergella* spp., *Macroglobigerinelloides* sp., *Praeglobotruncana gibba*, *Praeglobotruncana* sp., and *Archaeoglobigerina cretacea* (13–25, 33–34, 38–42, 50–51, 53, and 59 in Figure S2 and 7–10, 13–14, 18–20 in Figure S3). The fauna belongs to the *helvetica* zone of the Lower-Middle Turonian.

Autochthonous Cenomanian–Turonian sequences are known from the central Sakarya Basin and from the Haymana region (Figure 2; Yilmaz, 2008; Okay & Altıner, 2016; Ocağolu et al., 2018), where they are represented by a less than 100-m-thick sequence of pelagic limestone, marl, and shale.

4.2.8. Tuff, Radiolarian Chert, Sandstone, Siltstone, and Shale

These lithologies make up less than 6% of the blocks in the Alacaatlı Olistostromes. Most common are volcanogenic sandstone, siltstone, and shale blocks, which represent intrabasinal sediments reworked into the olistostromes during their emplacement. Green tuff blocks, 5 cm to 1 m across, consist of altered volcanic glass and form the most common noncarbonate blocks (Figure 4c); based on the zircon U–Pb dating of the intrabasinal volcanogenic sandstones, the tuffs are probably Albian in age (see section 4.4). Red radiolarian chert blocks, generally a few meters across, are widely distributed (Figure 5d); they also form an important component of the ophiolitic blocks.

4.3. Ophiolitic Blocks

The major ophiolitic mélangé belt in the Ankara region is located east of the Karakaya Complex, where it defines the İzmir-Ankara Suture (Figure 2). There is also a narrower and discontinuous second belt west of Ankara, where it is in contact with the Alacaatlı Olistostromes. This second belt was studied in the Alcı and Bağlum areas.

4.3.1. Ophiolitic Blocks in the Alcı Area

In the Alcı area the ophiolitic blocks crop out over a lens-shaped area between the Alacaatlı Olistostromes and the Campanian sequence (Figure 6; Koçyiğit, 1991; Rojay & Süzen, 1997). The blocks consist, in order of decreasing abundance, of red radiolarian chert, pelagic limestone, basalt, and rare blocks of phyllite and shallow marine limestone. Previous studies have interpreted the contact between the “ophiolitic mélangé” and the underlying Alacaatlı Olistostromes as a thrust fault (Koçyiğit, 1991; Rojay, 2013; Rojay & Süzen, 1997). However, the following lines of evidence indicate that the ophiolitic mélangé represents sedimentary mass flows, and has a depositional contact with the underlying Alacaatlı Olistostromes: (a) no clear-cut tectonic contact can be mapped in the field between the ophiolitic mélangé and the Alacaatlı Olistostromes. The contact is irregular with an increase in the red radiolarian chert blocks toward the ophiolitic mélangé, as seen in the Google Earth image in Figure 10a. (b) Red radiolarian chert blocks, which are the dominant ophiolite block type, also occur in the Alacaatlı Olistostromes; alternatively, radiolarian biomicritic limestones are common as block types in the ophiolitic mélangé. There is a mixing of the two block types

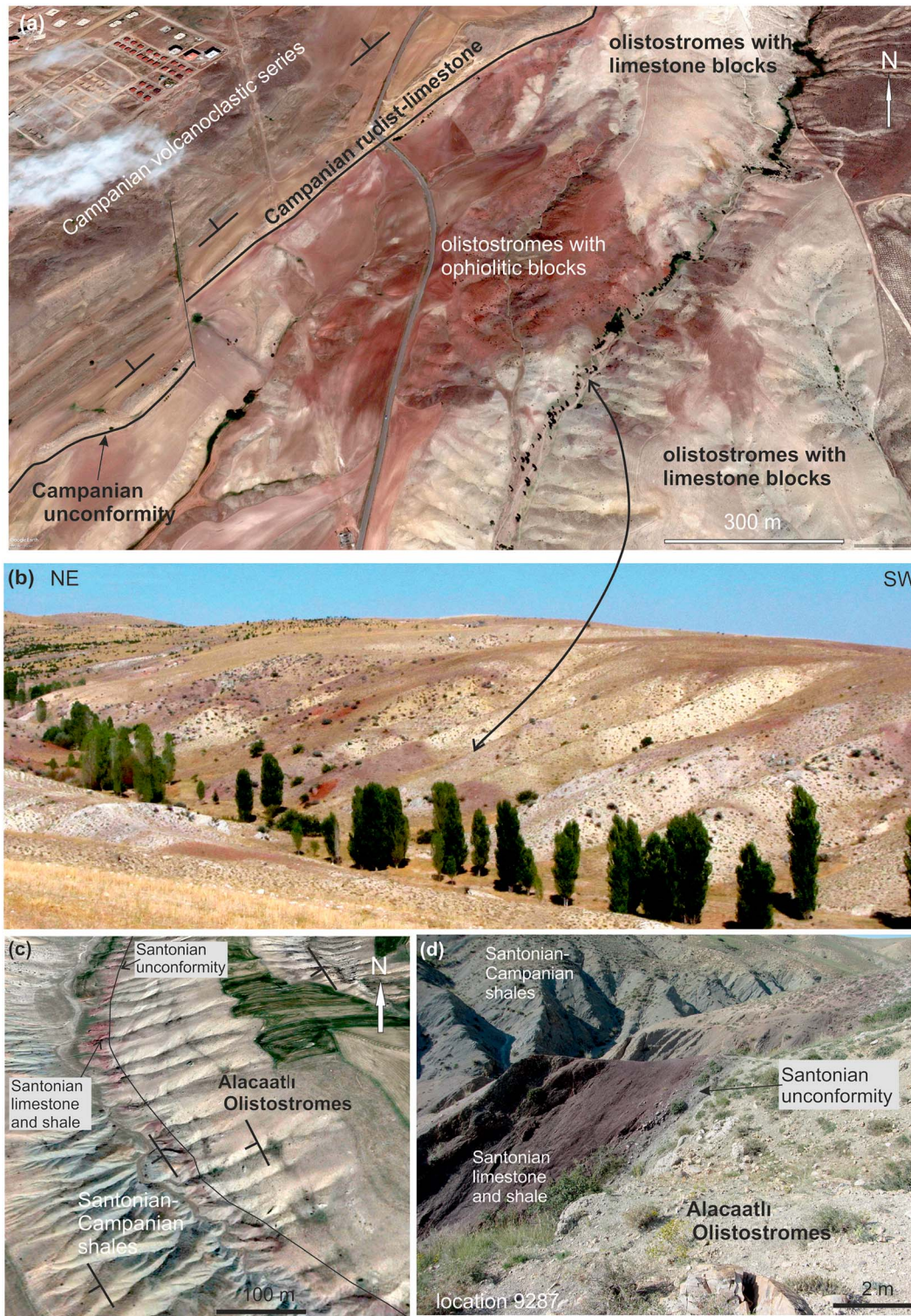


Figure 10. Alacaatlı Olistostromes, the ophiolitic mélangé, and the Santonian sequence in the Alçı region. (a) Google Earth image of the ophiolitic mélangé (red) and the surrounding Alacaatlı olistostromes (white). Note the irregular, interfingering boundary between the two units, which excludes a thrust contact. (b) Field photo of the contact zone between the Alacaatlı Olistostromes and the ophiolitic mélangé. Note the mixing of the limestone (white) and ophiolitic (red) blocks, location 9293. The double arrow indicates the location of the photograph in the Google Earth image. (c) Google Earth image of the unconformable boundary between the Alacaatlı Olistostromes and the overlying Santonian red limestones and shale. Note the truncation of the flow lines in the Alacaatlı Olistostromes by the Santonian sequence. (d) Santonian red shales over the olistostromes. For locations see Figure 6.

in the contact zone (Figure 10b). (c) Within the area mapped as ophiolitic *mélange*, there are breccias with clasts, 5–20 cm across, of red radiolarian chert and red limestone. We interpret the contact between the ophiolitic *mélange* and the Alacaatlı Olistostromes as stratigraphic and the ophiolitic *mélange* as sedimentary mass flows with ophiolitic blocks.

4.3.2. Ophiolitic *Mélange* in the Bağlum Area

Ophiolitic *mélange* in the Bağlum area crops out over a large area and is stratigraphically overlain by the Campanian turbidites (Figure 7; Gökten et al., 1988; Koçyiğit et al., 1988; Koçyiğit, 1991). It consists of basalt, radiolarian chert, shale, serpentinite, and limestone. Basalt makes up about 70% of the outcrops, followed by red radiolarian chert and red mudstone (15%), serpentinite (8%), and limestone (7%). In the field a block-matrix relation is not obvious; rather, the different lithologies are juxtaposed without an all-encompassing matrix. In places the ophiolitic *mélange* has a rough internal fabric defined by the parallel alignment of the limestone blocks. Compared to the Alcı region the olistostromal character of the ophiolitic *mélange* in the Bağlum area is generally less obvious. However, there is no evidence of faulting (e.g., cataclasis or mylonitization) along the well-exposed 2-km-long contact between the Alacaatlı Olistostromes and the ophiolitic *mélange* (Figure 7).

In the north the ophiolitic *mélange* is overlain unconformably by the Campanian turbidites. In this region the ophiolitic *mélange* is clearly olistostromal with blocks of basalt, chert, and limestone in a sandy-silty matrix (Koçyiğit, 1991). Based on these observations we interpret the ophiolitic *mélange* in the Bağlum area also as olistostromes.

Bragin and Tekin (1996) described a small outcrop of ophiolitic *mélange*, about 100 m across, surrounded by Neogene sediments west of Bağlum (Figure 2). The outcrop revisited during this study consists of microgabro, radiolarian chert–mudstone, and pelagic limestone blocks in a silty-sandy matrix. Within this small outcrop Bragin and Tekin (1996) describe individual radiolarian chert blocks of Late Triassic (Norian), Early Jurassic, Late Jurassic (Kimmeridgian-Tithonian), and Cretaceous (Albian-Turonian) ages. The mixing of radiolarian cherts of different ages points to a sedimentary origin of this ophiolitic *mélange* since in a typical subduction–accretion complex one would expect a younging toward the trench but uniform ages in small areas.

4.4. The Matrix of the Alacaatlı Olistostromes

The blocks in the Alacaatlı Olistostromes are surrounded by silt, clay, fine sand, and marl. The matrix makes up about 15–20% of the olistostromes and the blocks are generally matrix supported. Using sieve analysis Olgun and Norman (1993) found the matrix in the Alcı area to be sand-sized with a range of 0.2–0.5 mm. Most of the matrix is derived from the diminution of the incompetent blocks, including marls and marly limestone, and intrabasinal sandstone, siltstone, and shale beds. No cleavage or lineation is observed in the matrix.

4.5. Intrabasinal Sediments

Olistostrome flows are separated by intrabasinal sequences of medium-bedded to thinly bedded mudstone, shale, siltstone, sandstone, and marl, which makes up about 15% of the Alacaatlı Olistostromes (Figure 11). The thickness of such horizons ranges from a few meters to over hundred meters; some of the thicker intrabasinal horizons are shown in the geological maps in Figures 6 and 9. The dominant and distinctive lithology in the intrabasinal sediments is laminated red, purple mudstone, and siltstone (Figure 11). The lateral continuity of the intrabasinal sediment horizons was disrupted by the arrival of new mass flows, which erode these less cemented sediments and incorporate them as the matrix to the olistostromes. A stratigraphic section was measured in the thickest intrabasinal horizon (Figure 14b). The sequence consists of shale, mudstone, and siltstone horizons a few ten meters thick, which are intercalated with turbiditic volcanoclastic sandstone–shale horizons of similar thickness. Petrographically sandstone beds (9843B, 11266) consist of volcanic (70% of the clasts) and micritic limestone (30%) clasts. The carbonate clasts include Lower Cretaceous (Berriasian) limestones with *Calpionella alpina*, *Tintinopsella carpathica*, and *Calpionellopsis* sp., and Upper Cretaceous (Turonian-Santonian) clasts with *Marginotruncana pseudolinneiana*, *M. renzi*, *M. marginata*, and *Muricohedbergella delrioensis* (sample 9845C, 9–10, 13–14, and 20–21 in Figure S2). The mudstones contain, beside abundant radiolaria, *Muricohedbergella planispira*, *Heterohelix moremani*, and *Muricohedbergella hoelzli* (41, 44–45, and 50–51 in Figure S2), which indicate a Turonian and older Late

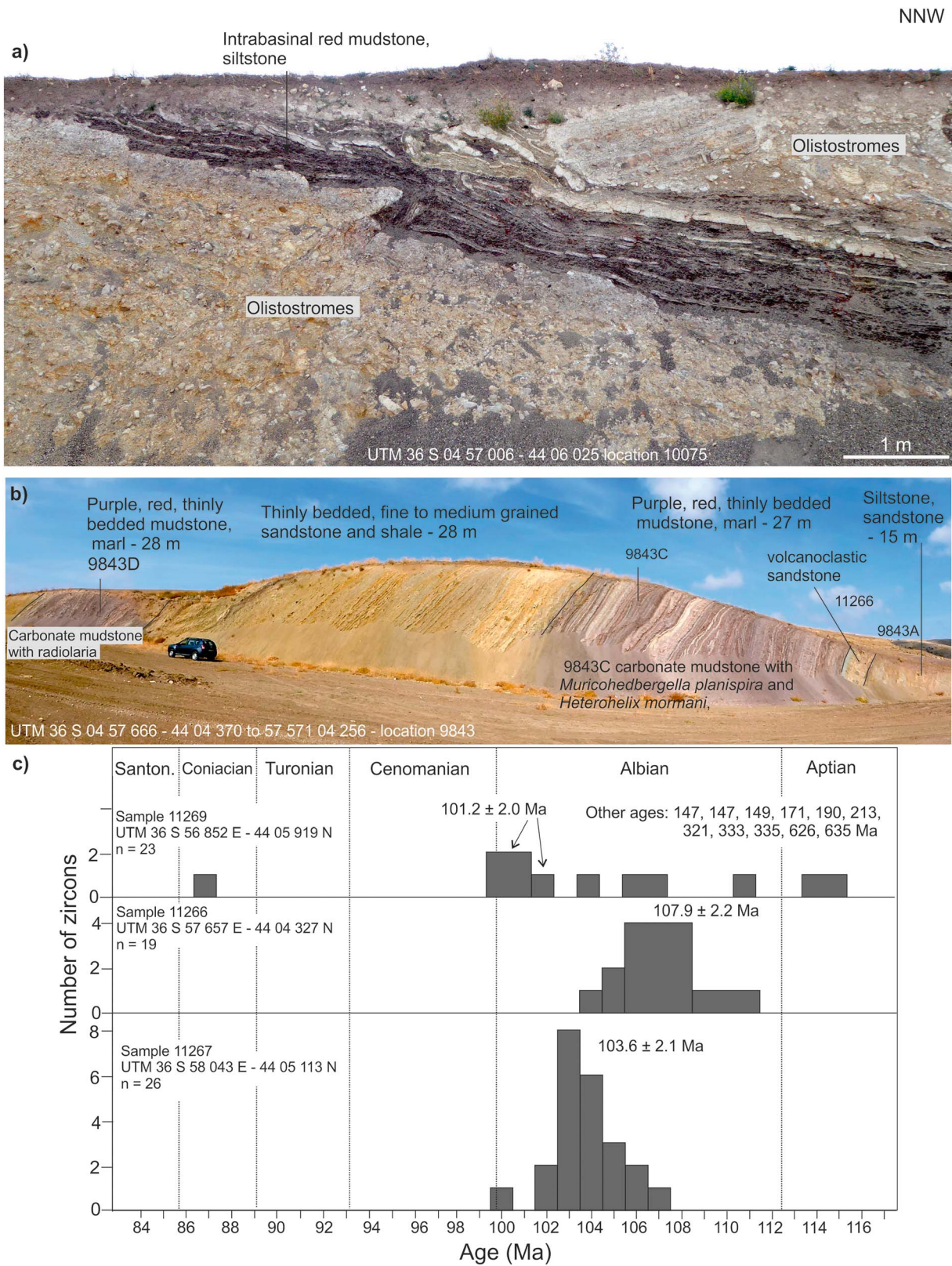


Figure 11. Intrabasinal sediments and their detrital zircon ages in the Alci area. (a) The 1-m-thick layer of carbonate mudstone and siltstone separating two olistostrome horizons. Note the drag fold which indicates northward (10°) movement. (b) The thickest horizon of intrabasinal sediments. (c) Histograms showing detrital zircon U-Pb ages from the intrabasinal volcanoclastic sandstones. For analytical data see Table S1.

Cretaceous age. Apart from this measured section, 21 samples from the intrabasinal mudstones and calcareous mudstones were studied to establish the age of the Alacaatlı Olistostromes. The samples are poorly fossiliferous; apart from widespread radiolaria they contain *Muricohedbergella planispira*, *Heterohelix moremani*, and *Muricohedbergella hoelzli*. One sample contains *Muricohedbergella holmdelensis* (43 in Figure S2), whose first occurrence is known from the Coniacian.

Detrital zircons from volcanoclastic sandstone beds in the intrabasinal sediments were dated using U–Pb single-grain laser ablation technique to constrain the age of magmatism. Two of the samples (11266 and 11267) come from the thickest intrabasinal horizon (Figure 6); they are composed mainly of andesite clasts and minor carbonate grains including microfossil fragments. Zircons from these samples are Albian with peaks at 107.9 ± 2.2 and 103.6 ± 2.1 Ma (Figure 11c and Table S1). The other sample (11269) comes from a stratigraphically higher intrabasinal horizon (Figure 6). It is composed of micritic limestone and volcanic clasts in equal proportion. One of the limestone clasts contains *Marginotruncana* sp., indicating a Turonian and younger depositional age. Zircons from this sample show a more heterogeneous age distribution (Figure 11c); Albian zircons are again dominant but are accompanied by Jurassic, Triassic, Carboniferous, and Neoproterozoic zircons. Significantly one zircon grain has yielded a Coniacian age of 87 ± 3 Ma (Table S1) in line with the age of the olistostromes.

Albian volcanoclastic sandstones are reported from the central Sakarya Basin (Yilmaz, 2008); however, Albian magmatic rocks are not known from the Pontides (Akdoğan et al., 2017). The virtual absence of Cenomanian to Coniacian zircons in the intrabasinal sediments indicates lack of contemporaneous magmatism, which is in keeping with the stratigraphic sequence in the central Sakarya Basin, where magmatism starts in the Campanian.

4.6. Volume and Transport Direction of the Olistostromes

The Alacaatlı Olistostromes crop out discontinuously for 112 km along strike from Dereköy in the south to the Mira mountain (Figure 2). The outcrops most likely form a continuous belt under the Neogene cover. The maximum outcrop width is 10 km, as observed in the Alacaatlı region; this would give a minimum surface area of 1,120 km². The maximum stratigraphic thickness of 2 km is observed in the Alcı region, which would indicate a volume of 2,240 km³; this would be a minimum value since the olistostromes extend northwest under the Campanian turbidite sequence (Figures 4 and 7). Submarine mass flows of similar and larger dimensions are described from several present-day continental margins (e.g., Torelli et al., 1997; Hjelstuen et al., 2007; Moscardelli & Wood, 2016) but are rare in the geological record.

Direct data on the transport direction of the debris flows are rare. Soft sediment structures include rare drag (slump) folds of the intrabasinal sediments (Figure 11a), and they generally indicate transport toward NNE in present coordinates (Figure 6). The wide and continuous belt of Upper Triassic Karakaya basement to the east of the olistostromes presently devoid of the Jurassic–Cretaceous cover (Figure 2) is a probable source of the Jurassic–Cretaceous limestone blocks. The ophiolitic blocks must also have been derived from the southeast (in present coordinates), where the Tethyan ocean was located in the Coniacian.

5. Santonian Sedimentation and Campanian Deformation

In the Alcı area the Alacaatlı Olistostromes are disconformably overlain a thin sequence of red micritic limestone and red shale (Figures 6 and 10d). The red limestone–shale sequence is about 15 m thick and crosscuts the flow lines in the underlying Coniacian olistostromes (Figure 10c). Eight samples from the red limestones contain planktonic foraminifera characteristic for the middle–late Santonian: *Dicarinella concavata*, *D. asymetrica*, *Marginotruncana pseudolinneiana*, *M. coronata*, *Globotruncanita elevata*, *G. bulloides*, *G. linneana*, *G. arca*, *G. lapparenti*, *Macroglobigerinelloides bollii*, *Muricohedbergella flandrini*, *Heterohelix globulosa*, and *H. reussi* (46 in Figure S2 and 1–6, 11–17, and 23–25 in Figure S3). The Santonian limestone–shale sequence passes up into red, bluish gray shale and mudstone with thin sandstone beds. The sequence, which has a minimum thickness of 65 m, has been dated to the latest Santonian to early–middle Campanian (*Globotruncanita elevata* zone) by planktonic foraminifera (Sariaslan & Altiner, 2017).

After the deposition of the Santonian sequence the region was deformed by folding, uplifted and eroded. The folding is recorded in the Santonian limestone and shale sequence, which forms NNE trending anticlines

and synclines (Figure 6). This period of contractional deformation was followed by the deposition of a Campanian sequence.

6. Campanian Sequence

In the Alcı area the folded Alacaatlı Olistostromes and ophiolitic mélangé are unconformably overlain by an Upper Cretaceous sequence (Figure 6; Koçyiğit, 1991; Koçyiğit & Lünel, 1987; Rojay & Süzen, 1997). The sequence starts with a fluvial red mudstone, siltstone, and conglomerate, up to 20 m in thickness, which are overlain by bluish gray shale and siltstone with bivalves, brachiopods, gastropods, and corals of the type *Cyclolites* sp.; ostracods from these clastic rocks indicate a Santonian-Campanian age range (Gizli, 2017). The shale and siltstones pass up into argillaceous limestones and then into thickly bedded, massive white to light gray limestones with abundant rudists. The rudist-bearing massive limestones, 6 to 30 m in thickness, can be followed as a marker horizon 11 km along strike (Figure 6). They are regarded as Maastrichtian (Koçyiğit, 1991; Koçyiğit & Lünel, 1987; Rojay & Süzen, 1997); however, we found the Campanian benthic foraminifera *Pseudosiderolites* sp. along with *Orbitoides* sp. in the rudist-limestones (samples 10059 and 10738B). Toward the top of the sequence the rudist-limestones contain clasts of biotite and feldspar. Fresh biotites from a 1.5-m-thick impure limestone bed (sample 9647) produced an Ar-Ar age of 76.8 ± 1.9 Ma (Figure 12d and Table S2), which is compatible with the Campanian age of the rudist-limestones.

The rudist-limestones in the Alcı area are overlain by a 750-m-thick sequence of volcanoclastic sandstone, siltstone, shale, tuff, and agglomerate with lenses of rudist-limestone, which is regarded as Paleocene in age (Koçyiğit & Lünel, 1987; Figure 13). However, zircons from two volcanoclastic sandstones close to the base of the sequence produced identical Campanian ages of 76.5 ± 1.5 and 76.3 ± 1.5 Ma (based on 45 and 75 coherent zircon ages from the samples 9648 and 9824, respectively; Figure 13 and Table S1).

The Alcı volcanoclastic sequence has a similar age as the widespread Campanian-Maastrichtian fore-arc turbidites, the Haymana formation, which crops out in the Haymana and Bağlum regions, and in the central Sakarya Basin (Figures 2 and 3; Ünalán et al., 1976; Özcan & Özkan-Altner, 1997; Ocakoğlu et al., 2018). To test the correlation of the Alcı and Haymana formations and to establish the age of arc magmatism, we dated detrital zircons from two sandstone samples from the Haymana formation, 20 and 50 km south and southwest of the Alcı region, respectively (Figure 2). One-hundred-two detrital zircons out of 107 from a sandstone sample from east of Polatlı (sample 10301) gave Campanian ages (79–72 Ma; Figure 14 and Table S1); the peak age is 73.5 Ma and the oldest Cretaceous zircon is 79 ± 2 Ma. One-hundred-four detrital zircons were analyzed from the sandstone sample from the Haymana region, of which 28 are Cretaceous zircons, which are largely in the range of 75–72 Ma (Figure 14). Zircons from the Alcı and Haymana formations show a similar Cretaceous age pattern dominated by late Campanian (78–72 Ma) zircons and contain no Santonian zircons. Detrital zircon data suggest that the arc magmatism started in the Campanian, which is compatible with the virtual absence of Coniacian zircons in the intrabasinal sandstones of the Alacaatlı Olistostromes.

In the Bağlum area the Campanian-Maastrichtian turbidite sequence, more than 800 m in thickness, lies above the ophiolitic mélangé, above the Alacaatlı Olistostromes, and above the Upper Triassic Karakaya Complex (Figure 7; Gökten et al., 1988; Koçyiğit et al., 1988; Koçyiğit, 1991). At the base of the turbidites there are red laminated silty biomicrites and calciturbidites, 5 m in thickness. Calciturbidites contain an abundance of volcanic detritus (samples 10432A, B) and locally a rich planktonic foraminifera fauna of *Globotruncana bulloides*, *G. linneiana*, *G. cf. ventricosa*, *Radotruncana cf. calcarata*, *Heterohelix globulosa*, and *Muricohedbergella* spp. (15–16 and 26–27 in Figure S3). Of these *Radotruncana cf. calcarata* is a late Campanian form, whereas *Globotruncana ventricosa* is a zone fossil for the middle–late Campanian. Thus, the paleontological data confirm the late Campanian basal age of the turbidite sequence (Gökten et al., 1988; Koçyiğit et al., 1988), and show it to be of the same age as the volcanoclastic sequence in the Alcı area.

The Campanian-Maastrichtian turbidites of the Alcı and Bağlum areas constitute part of major fore-arc basins along the western margin of the Kırşehir Massif, which includes the Haymana, Tuz Gölü, and Ulukışla basins (Görür et al., 1998; Gürer et al., 2016). They have formed by east-west extension between the Kırşehir-Paleo-Galatian magmatic arcs and a west dipping subduction zone.

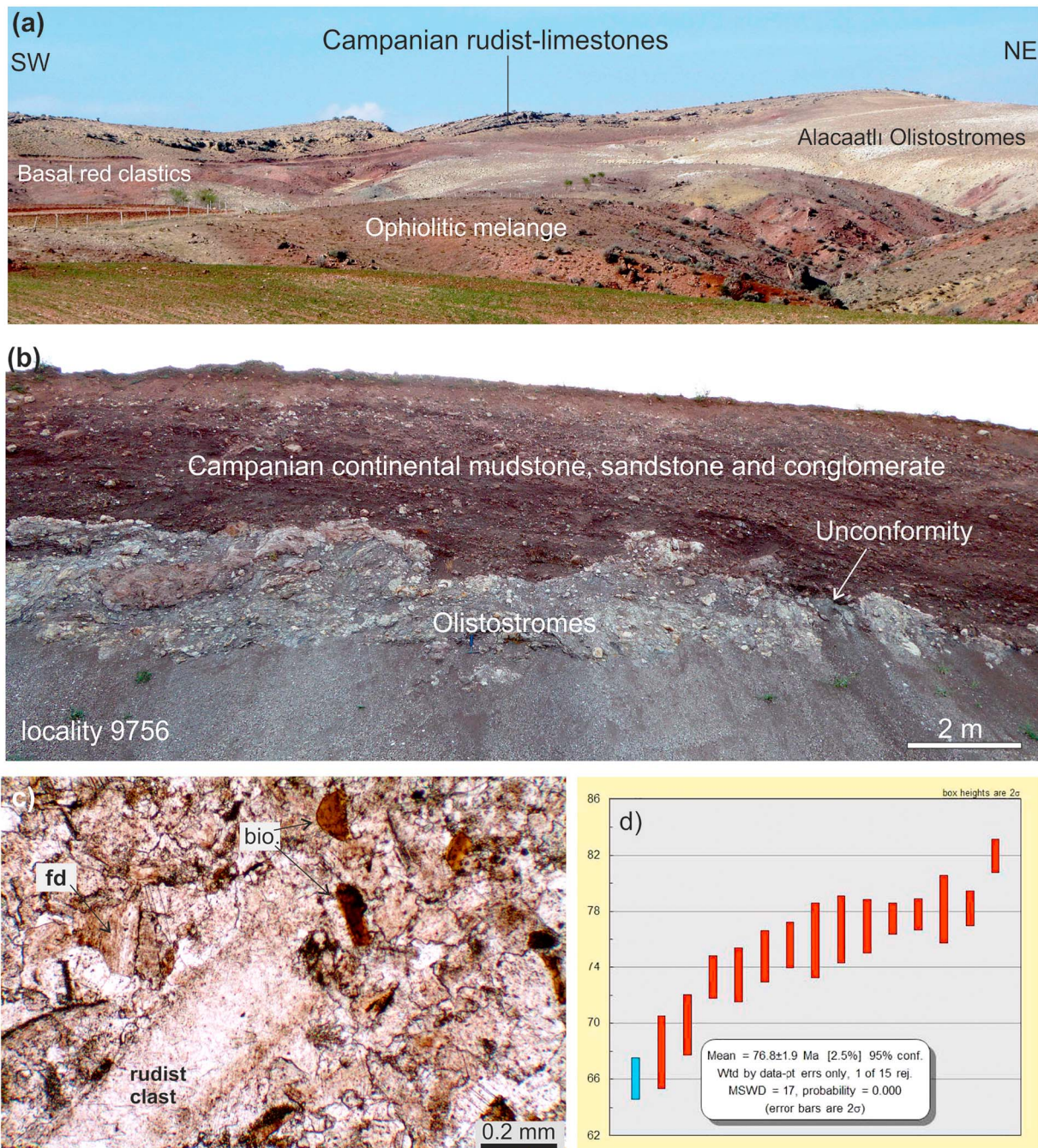


Figure 12. (a) Campanian red basal clastic rocks and rudist-limestones overlying unconformably the Alacaatlı Olistostromes and the ophiolitic mélange. (b) The unconformable contact between the red continental clastic rocks and the underlying Alacaatlı Olistostromes. This Campanian unconformity (82–77 Ma) corresponds to a phase of contractional deformation. (c) Photomicrograph in plane-polarized light of a limestone with rudist fragments, fresh feldspar (fd) and biotite (bio) clasts. Biotites from this sample (9647) produced an Ar–Ar age of 76.8 ± 1.9 Ma, which is shown in (d). For analytical data see Table S2.

7. Campanian Beypazarı Granite : Paleo-Galatian Magmatic Arc

A large Upper Cretaceous pluton, the Beypazarı Granite, with a geochemistry compatible with a magmatic arc setting (Figure 1; Öztürk et al., 2012; Speciale et al., 2014), crops out northwest of the Alacaatlı Olistostromes (Figures 1 and 3). The extent of the Late Cretaceous magmatism west of Ankara is obscured by the young cover; however, a small inlier of Campanian volcanic rocks (approximately 76 Ma), south of Kızılcahamam (Figure 2; Koçyiğit et al., 2003), and andesites (approximately 73 Ma) northwest of

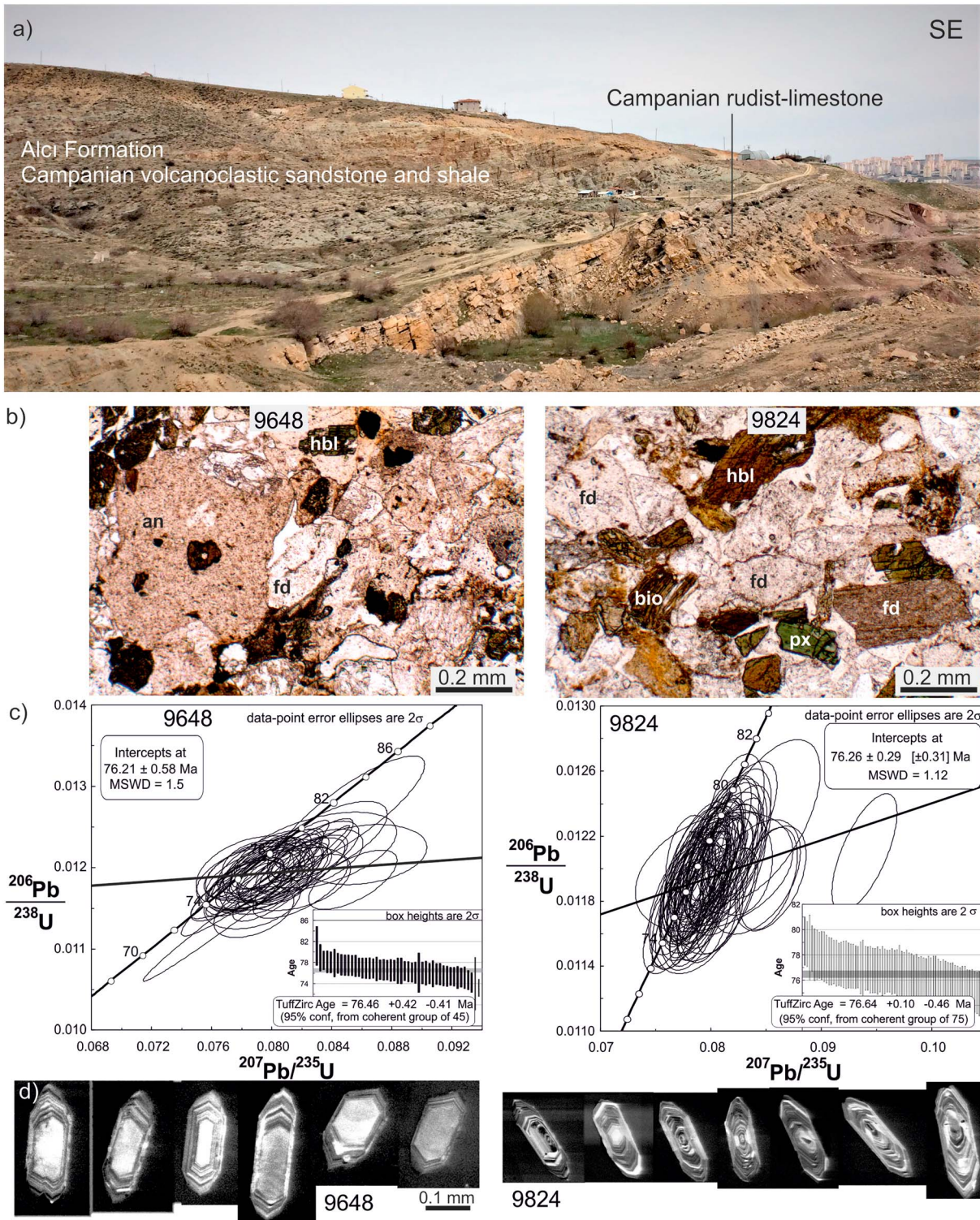


Figure 13. Alci formation. (a) Volcaniclastic sandstone and shale of the Alci formation lying above the rudist-limestones. (b) Photomicrographs of two dated sandstone samples (9648 and 9824) from the Alci formation consisting of andesite clasts (an), feldspar (fd), hornblende (hbl), biotite (bio), and pyroxene (px) grains. (c and d) Zircon U-Pb ages and zircon cathodoluminescence (CL) images from the same samples. For analytical data see Table S1.

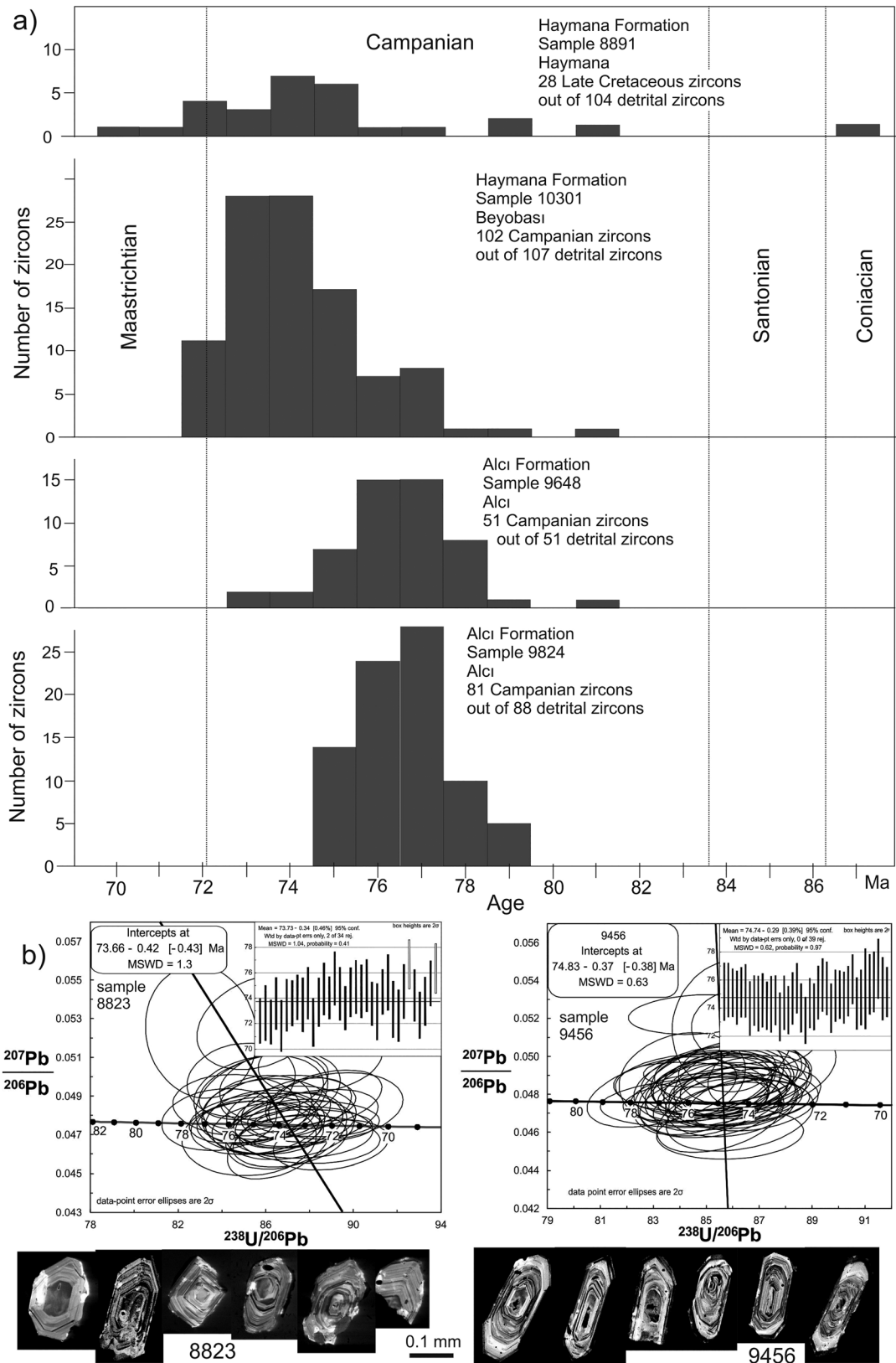


Figure 14. Zircon U-Pb data for Cretaceous arc magmatism. (a) Histograms of Cretaceous detrital zircons from the Campanian-Maastrichtian forearc sandstones (Haymana and Alci formations). (b) U-Pb concordia diagrams and CL images of zircons from the Beypazari granite. For location of the samples see Figure 3, and for the analytical data see Table S1.

Kızılcahamam (Keller et al., 1992) suggest that the Late Cretaceous magmatic belt, interpreted as a magmatic arc by Koçyiğit (1991), extends northeast subparallel to the İzmir-Ankara suture. This Paleogalatian magmatic arc, not to be confused with the Miocene Galatian volcanic province (e.g., Varol et al., 2014), is separate and highly oblique to the east-west trending Pontide magmatic arc (Figure 1).

Helvacı et al. (2014) provided 75 ± 2 -Ma U–Pb zircon ages from four samples of the Beypazarı Granite, whereas ion microprobe U–Pb zircon dating in thin section produced a wide range of ages from 92 down to 62 Ma for the same pluton (Speciale et al., 2014). To solve this apparent anomaly, we have dated zircons from two samples of the Beypazarı Granite using laser ablation ICP-MS technique. The results, based on over 30 individual zircon ages from each sample, are 74.8 ± 0.4 and 73.8 ± 0.4 Ma (Figure 14). Out of 81 individual concordant zircon ages obtained, 76 were between 72 and 76 Ma, and none were older than 80 Ma. The new zircons ages overlap with those from Helvacı et al. (2014) over a narrow range. It is also geologically implausible that parts of the Beypazarı Granite, which is a medium-sized, homogeneous pluton, cooled below 800–1,000 °C (the zircon closure temperature) at 92 Ma, and other parts 30 million years later at 62 Ma, as the data of Speciale et al. (2014) would imply. Therefore, we conclude that the Beypazarı Granite crystallized at 74 ± 2 Ma in the Campanian in line with the ages obtained from the volcanic rocks (Keller et al., 1992; Koçyiğit et al., 2003).

The best record for the onset and duration arc magmatism lies in the fore-arc basins (e.g., Sharman et al., 2015). The Campanian-Maastrichtian fore-arc turbidites west of Ankara contain detrital zircons with ages ranging from 78 to 72 Ma (Figure 14), which indicates that the arc magmatism was initiated at approximately 78 Ma. The virtual lack of Cenomanian to Coniacian detrital zircons in the intrabasinal sediments of the Alacaatlı Olistostromes (Figure 11) is a further support for the initiation of the arc magmatism in the Campanian.

8. Discussion

8.1. Olistostromes as Mass Flows

The chaotic internal structure and very poor sorting the Alacaatlı Olistostromes, the dominance of matrix supported blocks, and lack of any tectonic deformation indicate that the Alacaatlı Olistostromes were produced by mass flows. The lack of preferred orientation of the blocks and absence of syndepositional planar fabrics in the matrix, such as slump folds, indicate that the shear stress within the debris flows did not exceed the yield strength of the debris (Middleton & Hampton, 1973), which is in keeping with the large thicknesses of individual flows.

8.2. Age of the Debris Flows and the Origin of the Blocks

The youngest blocks in the Alacaatlı Olistostromes are late Turonian (92–90 Ma); the olistostromes are unconformably overlain by Santonian pelagic limestones (86–84 Ma). The youngest foraminifera and youngest zircon in the intrabasinal sediments is Coniacian (90–86 Ma); these data indicate that the Alacaatlı Olistostromes formed in the Coniacian (90–86 Ma).

Over 90% of the blocks in the Alacaatlı Olistostromes are limestone. Paleontological determinations show the presence of Callovian-Oxfordian, Tithonian, Berriasian, Valanginian, Aptian, Albian, Cenomanian, and Turonian limestone blocks. The blocks can be unambiguously assigned to the distal parts of the autochthonous Jurassic-Cretaceous sequence of the Sakarya Zone as exposed in the central Sakarya Basin and in the Haymana area (Figures 2 and 3; Rojay & Süzen, 1997). Over 95% of the limestone blocks are of pelagic character characterized by planktonic foraminifera. This indicates that the deep marine Jurassic-Cretaceous sequence of the Sakarya Zone was detached and transported into the Coniacian debris flows.

8.3. Constraining Features

There are a number of features of the Alacaatlı Olistostromes, which have a bearing on their tectonic setting and mechanism of their generation:

1. Uplift and erosion prior to the deposition of the olistostromes. The Alacaatlı Olistostromes lie stratigraphically above a substratum consisting of the Upper Triassic Karakaya Complex or over the Lower Jurassic sandstones. An intervening 2-km-thick pelagic carbonate sequence of Jurassic-Cretaceous age is missing. This Jurassic-Cretaceous section, which is well developed in the neighboring Haymana region and the central Sakarya Basin (Figure 3), must have been stripped before the deposition of the Alacaatlı Olistostromes.

2. Older blocks at the base. If a stratigraphic section is going to be reworked into olistostromes, one would expect the debris flows with the youngest blocks to occur in the base of the olistostromal sequence. However, in the Alacaatlı Olistostromes there is a general tendency for the older blocks to be in the lower stratigraphic levels, as for example the breccias with the greywacke clasts at the base of the Alacaatlı Olistostromes in the Bağlum area, or the large Tithonian-Berriasian limestone blocks close to the base of the Alacaatlı Olistostromes in the Alçı area.
3. Mixing of small blocks of different ages. Among the smaller blocks, there is a mixture of block ages even in a single outcrop. For example, an outcrop in the Alçı region just below the Santonian limestones has limestone blocks of Tithonian-Berriasian (sample 10267B), Albian (10267D), Cenomanian (10267C), and late Turonian (10266) ages. The 100-m-long ophiolitic mélange outcrop described by Bragin and Tekin (1996) has radiolarian chert and mudstone blocks of Late Triassic, Jurassic, and Early Cretaceous ages. This suggests that mixing of the blocks occurred before their final deposition possibly due to more than one phase of transport.
4. Subsidence during deposition. The Turonian-Santonian pelagic carbonate section in the Haymana region has a thickness of 60 m (Okay & Altner, 2016), whereas the Alacaatlı Olistostromes with a narrower age range have a stratigraphic thickness of 2 km. This indicates tectonically induced crustal subsidence during the deposition of the mass flows.
5. Trend parallel to the suture. The Alacaatlı Olistostromes form a belt subparallel to the İzmir-Ankara suture (Figures 1 and 2), which suggests a genetic connection between the trend of the continental margin during the Coniacian and the generation of the olistostromes. The 112-km-long belt of the olistostromes also indicates that the source was linear.
6. Rapid erosion followed by redeposition. The youngest blocks in the Alacaatlı Olistostromes are uppermost Turonian (approximately 90 Ma) pelagic marly limestones with no evidence of syndepositional tectonics. The youngest zircon in the intrabasinal sediments is Turonian-Coniacian (87 ± 3 Ma). The olistostromes are unconformably overlain by middle-late Santonian (85–84 Ma) pelagic limestones. These data indicate that erosion and redeposition of the Mesozoic sequence occurred in a few million years in the Coniacian to possibly earliest Santonian (89–86 Ma) involving quick uplift and erosion of the deep shelf-slope sequence followed by rapid subsidence.
7. Arc magmatism follows olistostrome deposition. There is no evidence for coeval magmatism during the deposition of the olistostromes; the intrabasinal volcanoclastic sandstones contain predominantly Albian zircons. Upper Cretaceous sequences in the Haymana region and in the central Sakarya Basin are also free of volcanic detritus until the Campanian (Okay & Altner, 2016) and the Campanian-Maastrichtian fore-arc turbidites contain Campanian zircons (Figure 14). Therefore, magmatism in the Paleo-Galatian arc started in the Campanian (approximately 78 Ma) approximately 9 Myr later than the deposition of the olistostromes (Coniacian; 89–86 Ma).

8.4. Tectonic Trigger for the Alacaatlı Olistostromes

The Alacaatlı Olistostromes and the ophiolitic mélange were deposited in a single short tectonic event in the Late Cretaceous (Coniacian; 89–86 Ma) before the onset of Paleo-Galatian (approximately 78 Ma) arc magmatism. The absence of arc magmatism during the deposition of the olistostromes could be related to shallow subduction or to the absence of subduction. Shallow subduction commonly creates shortening in the overriding plate, which is not compatible with the presence of deep marine Cenomanian-Santonian sequences in the Ankara region. Arc magmatism starts when the sinking slab reaches a threshold depth (e.g., England et al., 2004; Stern, 2002). Age data from the Beypazarı granite and zircons from the fore-arc sandstones indicate that the Paleo-Galatian arc magmatism started at approximately 78 Ma. Assuming an average slab dip of 40° , trench-normal convergence rate of 2 cm/year, and an average 124-km slab depth below the volcanic arc (Stern, 2002), the initiation of subduction will predate arc magmatism by approximately 9 Myr, and will overlap the deposition of the Alacaatlı Olistostromes at 89–86 Ma. Hence, we suggest that the Alacaatlı Olistostromes were formed during subduction initiation.

Late Cretaceous of Anatolia witnessed arc magmatism, opening of the West Black Sea basin, closure of the Intra-Pontide Ocean and continental subduction; the temporal and spatial relation between these events and the relation of the different plates are complicated and controversial. Especially, the Late Cretaceous location of the Kırşehir Massif and the relation of the Kırşehir Cretaceous magmatic arc to the subduction

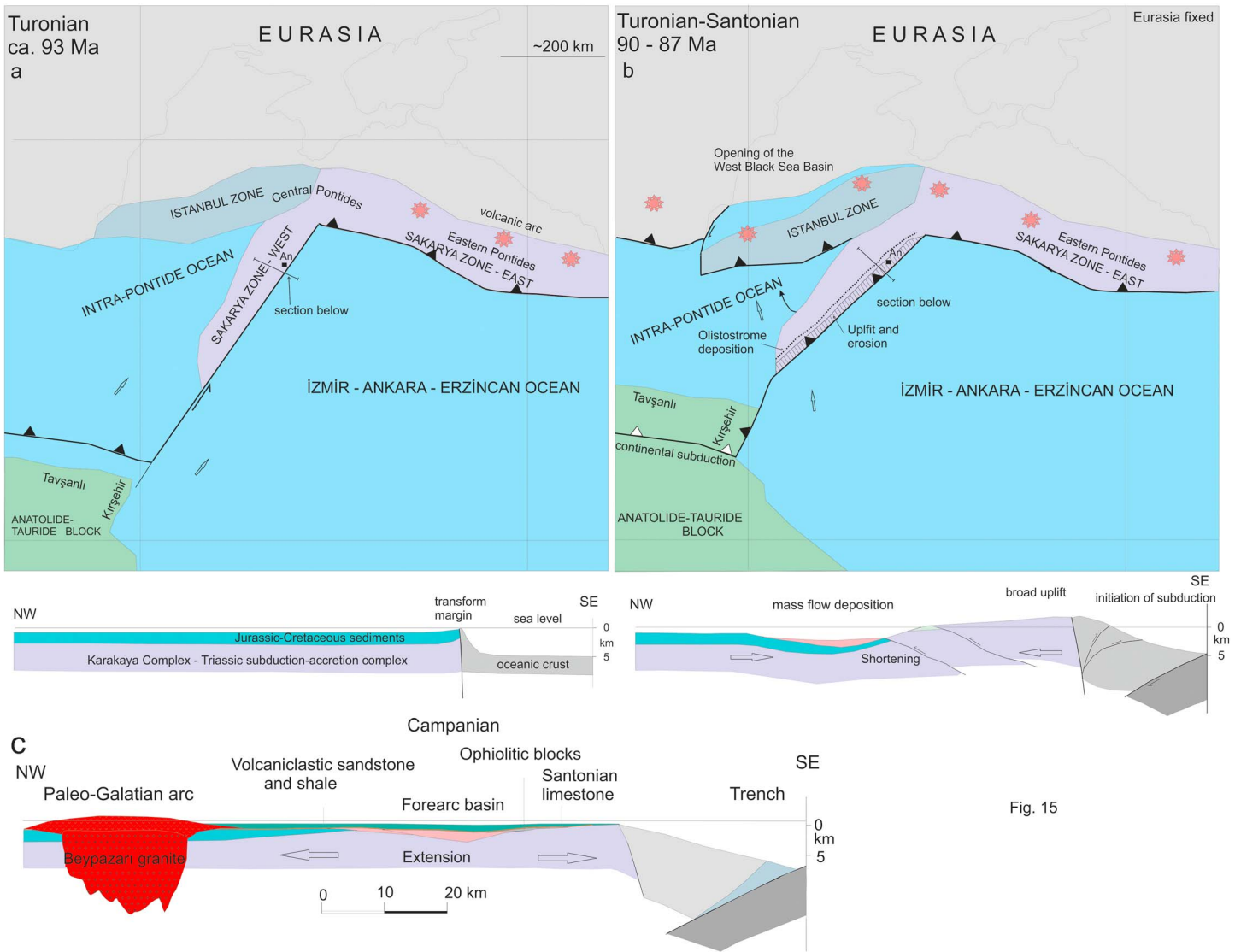


Figure 15. Paleogeography, plate boundary configuration, and cross sections of the Pontide realm and Tethys showing preferred mode of olistostrome generation through subduction initiation. An, Ankara. For details see the text.

zones, discussed above, are uncertain. The Kırşehir Massif is either regarded as an independent microcontinent in the Tethyan Ocean (e.g., Şengör et al., 1982; Whitney & Hamilton, 2004) or as part of the Anatolide-Tauride Block (e.g., Göncüoğlu et al., 1997; van Hinsbergen et al., 2016). A paleogeographic position of the Kırşehir Massif, east of the Tavşanlı Zone, as suggested by van Hinsbergen et al. (2016), would explain the Late Cretaceous ophiolite obduction observed in the Kırşehir Massif. However, recent paleotectonic models of van Hinsbergen et al. (2016) and Gürer et al. (2016) do not incorporate the Late Cretaceous closing of the Intra-Pontide Ocean and the opening of the oceanic West Black Sea basin, and envisage an east dipping subduction zone east of the Kırşehir Massif. Such a subduction configuration is not compatible with Late Cretaceous arc magmatism and high-temperature-low/intermediate-pressure metamorphism observed in the Kırşehir Massif. A paleotectonic model, which accounts for some of these features, is shown in Figure 15. A new feature in this reconstruction is the sharp bend of the Sakarya Zone at the central Pontides with the western Sakarya Zone oriented NNE. There are two lines of evidence for such an orientation: (a) the east-west trending Istanbul Zone and the eastern Sakarya Zone were amalgamated before the Late Jurassic in the central Pontides (Okay et al., 2018), whereas an oceanic embayment, the Intra-Pontide Ocean, existed between the Istanbul Zone and the western Sakarya Zone

until the latest Cretaceous; this necessitates a bend between the western and eastern Sakarya zones. (b) The arc magmatism in the western Sakarya Zone starts in the Campanian (approximately 78 Ma; e.g., Aysal et al., 2018). In contrast, there is ample evidence for earlier arc magmatism in the eastern Sakarya Zone (Eastern Pontides, 91–72 Ma; e.g., Aydınçakır, 2016; Eyuboglu, 2015; Kaygusuz et al., 2014; Liu et al., 2018; Özdamar, 2016). We suggest that the eastern margin of the western Sakarya Zone formed a transform fault (Figure 15), which linked the subduction under the Eastern Pontides to an intraoceanic subduction zone, which was initiated in the Turonian (approximately 93 Ma; Plunder et al., 2016). Such a configuration would explain the absence of arc magmatism, and hence subduction, during the Santonian in the Ankara region, when there was overall NNE-SSW convergence between Eurasia and Africa (Dewey et al., 1989; Rosenbaum et al., 2002; van Hinsbergen et al., 2016).

In the Santonian the northern promontory of the Anatolide-Tauride Block was pulled down in the intraoceanic subduction zone and underwent deformation and HP-LT metamorphism (Figure 15b). The continental subduction eventually blocked the intraoceanic subduction zone, and this most likely led to rejuvenated subduction or increased rate of subduction of the Intra-Pontide Ocean south of Istanbul Zone (Figure 15b). We suggest that subduction of the Intra-Pontide Ocean around a rotation pole located in the central Pontides, and rotational opening of the Western Black Sea basin led to a change from transform motion to oblique subduction along the eastern margin of the western Sakarya Zone (Figure 15b). The formation of the Alacaatlı Olistostromes is linked to this change from transform motion to oblique subduction. Subduction can initiate when a fracture zone or transform fault is under moderate compression (e.g., Hall et al., 2003; Stern & Gerya, 2018). During the Santonian-Campanian the proposed subduction geometry in the İzmir-Ankara ocean was similar to the present-day Japanese islands (e.g., Taira, 2001) with three subduction zones meeting at a triple point in the central Pontides.

Observations from Cenozoic subduction zones in the Pacific, such as the Puysegur trench (House et al., 2002) and geodynamic modeling (Gurnis et al., 2004), indicate that subduction initiation along a preexisting fault will induce uplift followed by subsidence in the overlying plate (cf. Stern, 2004). Modeling by Toth and Gurnis (1998) show a broad uplift of 1–2 km in the upper plate over a distance of 150 km away from the incipient trench. The wavelength of the uplift decreases to less than 70 km within a few million years but persists in regions close to the trench for over 10 Myr with a decreasing amplitude. The amount of rock uplift will be larger because of erosion leading to isostatic rebound not included in the model (Toth and Gurnis, 1998). The zone of uplift is bordered on the continent side by a rapidly subsiding trough reaching several kilometers in depth (cf. Figure 5a of Toth & Gurnis, 1998). In the case of the Western Sakarya margin the initial zone of broad uplift would be the 65-km-wide Triassic belt west of the İzmir-Ankara suture (Figure 2). In this belt the Jurassic to Late Cretaceous sedimentary cover is eroded probably in the early Coniacian. Later but still in the Coniacian, zone of uplift is reduced to 40 km bordered in the northwest by a rapidly subsiding trough, which received the Alacaatlı Olistostromes. The gradual decrease in the wavelength of uplift and increased subsidence inland of the uplift would have two consequences: (a) the regions of former uplift will receive sediments and debris flows from the uplift close to the trench and (b) some of the material will be retransported southeast.

By the late Santonian (84 Ma), the subduction system was relaxed with the deposition of pelagic carbonates and shales; this corresponds to a stage when the subduction becomes self-sufficient because of the negative buoyancy of the subducting oceanic lithosphere (e.g., Hall et al., 2003). The shortening and uplift at the beginning of the Campanian (approximately 80 Ma), a few million years before the start of arc magmatism (76 Ma), are difficult to explain, and may be related to the first large-scale generation of melts in the mantle wedge. A similar episode of uplift and shortening are observed before the start of the Pontide magmatism in the Cenomanian in the Eastern Pontides (Okay & Şahintürk, 1997). With the start of arc magmatism later in the Campanian (76 Ma), a wide fore-arc basin developed receiving volcanic detritus from the Paleogalatian arc.

9. Conclusions

A major mass flow event in central Anatolia occurred in a short interval in the Late Cretaceous (89–86 Ma), approximately 9 Myr before the start of the arc magmatism. It led to the deposition of olistostromes up to 2 km thick, which can be followed for more than 112 km along strike. The olistostromes consist of

Jurassic–Cretaceous pelagic limestone and subsidiary ophiolitic blocks in a clastic matrix; the pelagic limestone blocks have been derived from the Pontide continental margin. We ascribe the formation of mass flows to the destabilization of the continental margin associated with a change from transform motion to subduction. A number of peculiar features of the mass flows including the dominance of pelagic limestone blocks, uplift, and erosion before the deposition indicate shortening of the continental margin followed by the creation of a deep ephemeral basin. Shortening perpendicular to trench is caused by a change from transform margin to subduction. Subduction along this western Sakarya margin led to the formation of the northeast trending Paleo-Galatian magmatic arc, distinct from the east-west trending Pontide arc. Age data from the Beypazarı Granite, volcanic rocks, and from the detrital zircons data from the fore-arc sequence indicate that the Paleo-Galatian arc became active in the Campanian (approximately 78 Ma) later than the Pontide arc.

Acknowledgments

We thank Ercan Özcan for the determination of Campanian benthic foraminifera, Gürsel Sunal and Mesut Aygül for their help in geochronology, and Sarah Sherlock for the Ar–Ar dating. Comments by Douwe van Hinsbergen, Peter McPhee, and Derya Güner improved an earlier version of the model. This study was supported by the TÜBİTAK project 113R007 and partly by TÜBA. Data for this study are provided in the supporting information.

References

- Ager, D. V. (1959). Lower Jurassic brachiopods from Turkey. *Journal of Paleontology*, 33, 1018–1028.
- Akbayram, K., Okay, A. I., & Satır, M. (2013). Early Cretaceous closure of the Intra-Pontide Ocean in western Pontides (northwestern Turkey). *Journal of Geodynamics*, 65, 38–55. <https://doi.org/10.1016/j.jog.2012.05.003>
- Akdoğan, R., Okay, A. I., Sunal, G., Tari, G., Meinhold, G., & Kylander-Clark, A. R. C. (2017). Provenance of a large Lower Cretaceous turbidite submarine fan on the active Laurasian margin. *Journal of Asian Earth Sciences*, 134, 309–329. <https://doi.org/10.1016/j.jseaes.2016.11.028>
- Alkaya, F., & Meister, C. (1995). Liassic ammonites from the central and eastern Pontides (Ankara and Kelkit areas, Turkey). *Revue de Paléobiologie*, 14, 125–193.
- Altuner, D. (1991). Microfossil biostratigraphy (mainly foraminifers) of the Jurassic-Lower Cretaceous carbonate successions in North-Western Anatolia (Turkey). *Geologica Romana*, 27, 167–213.
- Altuner, D., Koçyiğit, A., Farinacci, A., Nicosia, U., & Conti, M. A. (1991). Jurassic-Lower Cretaceous stratigraphy and paleogeographic evolution of the southern part of North-Western Anatolia. *Geologica Romana*, 28, 13–80.
- Altuner, D., & Özkan, S. (1991). Calpionellid zonation in North-Western Anatolia (Turkey) and calibration of the stratigraphic ranges of some benthic foraminifera at the Jurassic-Cretaceous boundary. *Geologica Romana*, 27, 215–235.
- Altınlı, E. (1976). Geology of the northern portion of the Middle Sakarya River. *İstanbul Üniversitesi Fen Fakültesi Mecmuası, Seri*, 41, 35–56.
- Aydınçakır, A. (2016). Subduction-related Late Cretaceous high-K volcanism in the central Pontides orogenic belt: Constraints on geodynamic implications. *Geodinamica Acta*, 28(4), 379–411. <https://doi.org/10.1080/09853111.2016.1208526>
- Aysal, N., Keskin, M., Peytcheva, I., & Duru, O. (2018). Geochronology, geochemistry and isotope systematics of a mafic-intermediate dyke complex in the İstanbul zone. New constraints on the evolution of the Black Sea in NW Turkey. *Geological Society, London, Special Publications*, 464(1), 131–168. <https://doi.org/10.1144/SP464.4>
- Bailey, E. B., & McCallien, W. J. (1950). The Ankara Melange and the Anatolian thrust. *Nature*, 166(4231), 938–940. <https://doi.org/10.1038/166938a0>
- Bailey, E. B., & McCallien, W. J. (1953). Serpentine lavas, the Ankara melange and the Anatolian thrust. *Earth and Environmental Science Transactions of The Royal Society of Edinburgh*, 62(02), 403–442. <https://doi.org/10.1017/S008045680009340>
- Batman, B. (1978). Geological evolution of the region north of Haymana and the study of the mélange. I. Stratigraphic units (in Turkish). *Yerbilimleri*, 4, 95–124.
- Batman, B., Kulaksız, S., & Görmüş, S. (1978). A study of the deformational properties of the Jurassic-Cretaceous sequence in the Alacaatlı region (SW Ankara) (in Turkish). *Yerbilimleri*, 4, 135–152.
- Boccaletti, M., Bortolotti, V., & Sagri, M. (1966). Ricerche sulle ofioliti delle Catene Alpine. 1. Osservazioni sull'Ankara Melange nella zona di Ankara. *Bollettino della Società Geologica Italiana*, 85, 485–508.
- Bortolotti, V., Chiari, M., Göncüoğlu, M. C., Principi, G., Saccani, E., Tekin, U. K., & Tassinari, R. (2018). The Jurassic–Early Cretaceous basalt–chert association in the ophiolites of the Ankara Mélange, east of Ankara, Turkey: Age and geochemistry. *Geological Magazine*, 155(02), 451–478. <https://doi.org/10.1017/S0016756817000401>
- Bragin, N. Y., & Tekin, U. K. (1996). Age of radiolarian chert blocks from the Senonian ophiolitic melange (Ankara, Turkey). *Island Arc*, 5(2), 114–122. <https://doi.org/10.1111/j.1440-1738.1996.tb00018.x>
- Bragin, N. Y., & Tekin, U. K. (1999). Stratigraphy and the Upper Jurassic-Lower Cretaceous radiolarians from the carbonate-siliceous deposits, Ankara region, Turkey. *Stratigraphy and Geological Correlation*, 7, 130–140.
- Bremer, H. (1966). Ammoniten aus dem untereren Bajocium und unteren Bathonium in der Umgebung von Ankara (Türkei). *Neues Jahrbuch für Geologie und Paläontologie, Abhandlungen*, 125, 155–169.
- Çapan, U. Z., & Buket, E. (1975). Geology of the Aktepe-Gökdere region and the ophiolitic mélange (in Turkish). *Türkiye Jeoloji Kurumu Bülteni*, 18, 11–16.
- Çelik, Ö. F., Chiaradia, M., Marzoli, A., Billor, Z., & Robert, M. (2013). The Eldivan ophiolite and volcanic rocks in the İzmir–Ankara–Erzincan suture zone, northern Turkey: Geochronology, whole-rock geochemical and Nd–Sr–Pb isotope characteristics. *Lithos*, 172–173, 31–46.
- Dangerfield, A., Harris, R., Sarifakioglu, E., & Dilek, Y. (2011). Tectonic evolution of the Ankara Mélange and associated Eldivan ophiolite near Hançili Central Turkey. *Geological Society of America Special Papers*, 480, 143–169.
- Deli, A., & Orhan, H. (2007). Stratigraphy of Jurassic-Cretaceous aged deposits around Alacaatlı-Beytepe village (southwest Ankara) (in Turkish). *Journal Selçuk University Faculty of Engineering and Architecture*, 22, 61–80.
- Delibaş, O., Genç, Y., & de Campos, C. P. (2011). Magma mixing and unmixing related mineralization in the Karacaali Magmatic Complex, Central Anatolia, Turkey. *Geological Society, London, Special Publications*, 350(1), 149–173. <https://doi.org/10.1144/SP350.9>
- Dewey, J. F., Helman, M. L., Turco, E., Hutton, D. H. W., & Knott, S. D. (1989). Kinematics of the western Mediterranean. In M. P. Coward, D. Dietrich, & R. G. Park (Eds.), *Alpine Tectonics* (Vol. 45, pp. 265–283). Geological Society Special Publication.
- Dilek, Y., & Thy, P. (2006). Age and petrogenesis of plagiogranite intrusion in the Ankara melange, central Turkey. *Island Arc*, 15(1), 44–57. <https://doi.org/10.1111/j.1440-1738.2006.00522.x>
- England, P., Engdahl, R., & Thatcher, W. (2004). Systematic variation in the depths of slabs beneath arc volcanoes. *Geophysical Journal International*, 156, 377–408.

- Eyuboglu, Y. (2015). Petrogenesis and U–Pb zircon chronology of felsic tuffs interbedded with turbidites (eastern Pontides Orogenic Belt, NE Turkey): Implications for Mesozoic geodynamic evolution of the eastern Mediterranean region and accumulation rates of turbidite sequences. *Lithos*, 212–215, 74–92.
- Festa, A., Ogata, K., Pini, G. A., Dilek, Y., & Alonso, J. L. (2016). Origin and significance of olistostromes in the evolution of orogenic belts: A global synthesis. *Gondwana Research*, 39, 180–203. <https://doi.org/10.1016/j.gr.2016.08.002>
- Gizli, H. T. (2017). Ostracoda biostratigraphy, chronostratigraphy and paleoenvironmental interpretation of the Upper Cretaceous İncirli Formation in the Alcı-Aşağı Yurtçu region, southwest of Ankara. MSc thesis, Hacettepe University, Ankara. Retrieved from <http://www.openaccess.hacettepe.edu.tr:8080/xmlui/handle/11655/3109?show=full>
- Gökten, E., Kazancı, N., & Acar, Ş. (1988). Stratigraphy and tectonics of the Upper Cretaceous-Pliocene series northwest of Ankara (between Bağlum and Kazanı) (in Turkish). *Maden Tetkik ve Arama Dergisi*, 108, 69–81.
- Göncüoğlu, M. C., Dirik, K., & Kozlu, H. (1997). Pre-alpine and alpine terranes in Turkey: Explanatory notes to the terrane map of Turkey. *Annales Geologique de Pays Hellenique*, 37, 515–536.
- Görür, N., Tüysüz, O., & Şengör, A. M. C. (1998). Tectonic evolution of the central Anatolian basins. *International Geology Review*, 40(9), 831–850. <https://doi.org/10.1080/00206819809465241>
- Gürer, D., van Hinsbergen, D. J., Matenco, L., Corfu, F., & Cascella, A. (2016). Kinematics of a former oceanic plate of the Neotethys revealed by deformation in the Ulukışla Basin (Turkey). *Tectonics*, 35, 2385–2416. <https://doi.org/10.1002/2016TC004206>
- Gurnis, M., Hall, C., & Lavier, L. (2004). Evolving force balance during incipient subduction. *Geochemistry, Geophysics, Geosystems*, 5, Q07001. <https://doi.org/10.1029/2003GC000681>
- Hall, C. E., Gurnis, M., Sdrölias, M., Lavier, L. L., & Müller, R. D. (2003). Catastrophic initiation of subduction following forced convergence across fracture zones. *Earth and Planetary Science Letters*, 212(1–2), 15–30. [https://doi.org/10.1016/S0012-821X\(03\)00242-5](https://doi.org/10.1016/S0012-821X(03)00242-5)
- Helvacı, C., Öztürk, Y. Y., Satır, M., & Shang, C. K. (2014). U–Pb zircon and K–Ar geochronology reveal the emplacement and cooling history of the Late Cretaceous Beypazarı granitoid, Central Anatolia, Turkey. *International Geology Review*, 56(9), 1138–1155. <https://doi.org/10.1080/00206814.2014.921795>
- van Hinsbergen, D. J. J., Maffione, M., Plunder, A., Kaymakçı, N., Ganerød, M., Hendriks, B. W. H., et al. (2016). Tectonic evolution and paleogeography of the Kırşehir block and the central Anatolian ophiolites, Turkey. *Tectonics*, 35, 983–1014. <https://doi.org/10.1002/2015TC004018>
- Hjelstuen, B. O., Eldholm, O., & Faleide, J. I. (2007). Recurrent Pleistocene mega-failures on the SW Barents Sea margin. *Earth Planetary Science Letters*, 258(3–4), 605–618. <https://doi.org/10.1016/j.epsl.2007.04.025>
- House, M. A., Gurnis, M., Kamp, P. J. J., & Sutherland, R. (2002). Uplift in the Fiordland region, New Zealand: Implications for incipient subduction. *Science*, 297(5589), 2038–2041. <https://doi.org/10.1126/science.1075328>
- Kaygusuz, A., Arslan, M., Siebel, W., Sipahi, F., İlbeyli, N., & Temizel, İ. (2014). LA-ICP MS zircon dating, whole-rock and Sr–Nd–Pb–O isotope geochemistry of the Camiboğazi pluton, eastern Pontides, NE Turkey: Implications for lithospheric mantle and lower crustal sources in arc-related I-type magmatism. *Lithos*, 192–195, 271–290.
- Keller, J., Jung, D., Eckhardt, F. J., & Kreuzer, H. (1992). Radiometric ages and chemical characterization of the Galatean andesite massif, Pontus, Turkey. *Acta Vulcanologica*, 2, 267–276.
- Koçyiğit, A. (1987). The tectonostratigraphy of the Hasanoğlan (Ankara) region: The evolution of the Karakaya orogenic belt (in Turkish). *Yerbilimleri*, 14, 269–294.
- Koçyiğit, A. (1991). An example of an accretionary forearc basin from northern central Anatolia and its implications for the history of subduction of Neo-Tethys in Turkey. *Bulletin Geological Society of America*, 103(1), 22–36. [https://doi.org/10.1130/0016-7606\(1991\)103<0022:AEOAAF>2.3.CO;2](https://doi.org/10.1130/0016-7606(1991)103<0022:AEOAAF>2.3.CO;2)
- Koçyiğit, A., & Lünel, A. T. (1987). Geology and tectonic setting of Alcı region, Ankara. *Middle East Technical University, Journal of Pure and Applied Sciences*, 20, 35–57.
- Koçyiğit, A., Özkan, S., & Rojay, B. F. (1988). Examples from the forearc basin remnants at the active margin of northern Neo-Tethys: development and emplacement ages of the Anatolian Nappe, Turkey. *METU Journal of Pure and Applied Sciences*, 21, 183–210.
- Koçyiğit, A., Winchester, J. A., Bozkurt, E., & Holland, G. (2003). Saraçköy volcanic suite: Implications for the subductional phase of arc evolution in the Galatian arc complex, Ankara, Turkey. *Geological Journal*, 38(1), 1–14. <https://doi.org/10.1002/gj.921>
- Köksal, S., Romer, R. L., Göncüoğlu, M. C., & Toksoy-Köksal, F. (2004). Timing of post-collisional H-type to A-type granitic magmatism: U–Pb titanite ages from the alpine central Anatolian granitoids (Turkey). *International Journal of Earth Sciences*, 93(6), 974–989. <https://doi.org/10.1007/s00531-004-0432-5>
- Kuznetsova, K. I., Bragin, N. Y., Voznesenskii, A. I., & Tekin, U. K. (2003). Jurassic planktonic and benthic cosmopolitan foraminiferal communities of central Turkey. *Stratigraphy and Geological Correlation*, 11, 450–467.
- Kylander-Clark, A. R. C., Hacker, B. R., & Cottle, J. M. (2013). Laser-ablation split-stream ICP petrochronology. *Chemical Geology*, 345, 99–112. <https://doi.org/10.1016/j.chemgeo.2013.02.019>
- Lefebvre, C., Meijers, M. J. M., Kaymakçı, N., Peynircioğlu, A., Langereis, C. G., & van Hinsbergen, D. J. J. (2013). Reconstructing the geometry of central Anatolia during the late Cretaceous: Large-scale Cenozoic rotations and deformation between the Pontides and Taurides. *Earth Planetary Science Letters*, 366, 83–98. <https://doi.org/10.1016/j.epsl.2013.01.003>
- Liu, Z., Zhu, D.-C., Wang, Q., Eyuboglu, Y., Zhao, Z.-D., Liu, S.-A., & Xu, L.-J. (2018). Transition from low-K to high-K calc-alkaline magmatism at approximately 84 Ma in the eastern Pontides (NE Turkey): Magmatic response to slab rollback of the Black Sea. *Journal of Geophysical Research: Solid Earth*, 123, 7604–7628. <https://doi.org/10.1029/2018JB016026>
- Meijers, M. J. M., Kaymakçı, N., van Hinsbergen, D. J. J., Langereis, C. G., Stephenson, R. A., & Hippolyte, J. C. (2010). Late Cretaceous to Paleocene oroclinal bending in the central Pontides (Turkey). *Tectonics*, 29, TC4016. <https://doi.org/10.1029/2009TC002620>
- Mekik, F. A. (2000). Early Cretaceous Pantanelliidae (Radiolaria) from northwest Turkey. *Micropaleontology*, 46, 1–30.
- Mekik, F. A., Ling, H. Y., Özkan Altuner, S., & Altuner, D. (1999). Preliminary radiolarian biostratigraphy across the Jurassic-Cretaceous boundary from northwestern Turkey. *Geodiversitas*, 21, 715–738.
- Middleton, G. V., & Hampton, M. A. (1973). Sediment gravity flows: Mechanism of flow and deposition. In G. V. Middleton & A. H. Bouma (Eds.), *Turbidite and Deep Water Sedimentation, SEPM* (pp. 1–38). Pacific section, Short Course Lecture Notes.
- Moscaredelli, L., & Wood, L. (2016). Morphometry of mass-transport deposits as a predictive tool. *Geological Society of America Bulletin*, 128, 47–80.
- Nikishin, A. M., Okay, A. I., Tüysüz, O., Demirel, A., Wannier, M., Amelin, N., & Petrov, E. (2015). The Black Sea basins structure and history: New model based on new deep penetration regional seismic data. Part 2: Tectonic history and paleogeography. *Marine and Petroleum Geology*, 59, 656–670. <https://doi.org/10.1016/j.marpetgeo.2014.08.018>

- Öçakoğlu, F., Hakyemez, A., Açıkalın, S., Özkan Altın, S., Büyükerem, Y., Licht, A., et al. (2018). Chronology of subduction and collision along the İzmir-Ankara suture in Western Anatolia: Records from the central Sakarya Basin. *International Geology Review*, 1–26. <https://doi.org/10.1080/00206814.2018.1507009>
- Okay, A. I., & Altın, D. (2016). Carbonate sedimentation in an active margin: Cretaceous history of the Haymana region, Pontides. *International Journal of Earth Sciences*, 105(7), 2013–2030. <https://doi.org/10.1007/s00531-016-1313-4>
- Okay, A. I., Altın, D., Sunal, G., Tüysüz, O., Aygül, M., Akdoğan, R., et al. (2018). Geological evolution of the central Pontides. *Geological Society London Special Publications*, 464(1), 33–67. <https://doi.org/10.1144/SP464.3>
- Okay, A. I., & Gönçüoğlu, M. C. (2004). Karakaya complex: A review of data and concepts. *Turkish Journal of Earth Sciences*, 13, 77–95.
- Okay, A. I., & Nikishin, A. M. (2015). Tectonic evolution of the southern margin of Laurasia in the Black Sea region. *International Geology Review*, 57(5–8), 1051–1076. <https://doi.org/10.1080/00206814.2015.1010609>
- Okay, A. I., & Şahintürk, Ö. (1997). Geology of the eastern Pontides. In A. G. Robinson (Ed.), *Regional and Petroleum Geology of the Black Sea and Surrounding Region* (Vol. 68, pp. 291–311). American Association of Petroleum Geologists (AAPG) Memoir.
- Okay, A. I., Sunal, G., Tüysüz, O., Sherlock, S., Keskin, M., & Kylander-Clark, A. R. C. (2014). Low-pressure-high-temperature metamorphism during extension in a Jurassic magmatic arc, central Pontides, Turkey. *Journal of Metamorphic Geology*, 32(1), 49–69. <https://doi.org/10.1111/jmg.12058>
- Okay, A. I., & Tüysüz, O. (1999). Tethyan sutures of northern Turkey. In B. Durand, L. Jolivet, F. Horváth, & M. Séranne (Eds.), *The Mediterranean Basins: Tertiary extension within the Alpine orogen*, Geological Society, London, Special Publication 156 (pp. 475–515).
- Okay, A. I., & Whitney, D. L. (2010). Blueschists, eclogites, ophiolites and suture zones in northwest Turkey: A review and a field excursion guide. *Ophiolithi*, 35, 131–172.
- Olgun, E., & Norman, T. (1993). Grain size analyses of some olistostromes between Balkuyumcu and Alcı (SW Ankara). *Bulletin of the Mineral Research and Exploration*, 115, 31–48.
- Özcan, E., & Özkan-Altın, S. (1997). Late Campanian-Maastrichtian evolution of orbitoid foraminifera in Haymana basin succession (Ankara, central Turkey). *Revue de Paléobiologie*, 16(1), 271–290.
- Özdamar, Ş. (2016). Geochemistry and geochronology of late Mesozoic volcanic rocks in the northern part of the eastern Pontide Orogenic Belt (NE Turkey): Implications for the closure of the Neo-Tethys Ocean. *Lithos*, 248–251, 240–256.
- Öztürk, Y. Y., Helvacı, C., & Satır, M. (2012). Geochemical and isotopic constraints on petrogenesis of the Beypazarı Granitoid, NW Ankara, western central Anatolia, Turkey. *Turkish Journal of Earth Sciences*, 21, 53–77.
- Plunder, A., Agard, P., Chopin, C., Soret, M., Okay, A. I., & Whitechurch, H. (2016). Metamorphic sole formation, emplacement and blueschist overprint: Early obduction dynamics witnessed by Western Turkey ophiolites. *Terra Nova*, 28(5), 329–339. <https://doi.org/10.1111/ter.12225>
- Premoli Silva, L., & Verga, D. (2004). Practical manual of Cretaceous planktonic foraminifera. In D. Verga & R. Rettori (Eds.), *International School on Planktonic Foraminifera, 3^o Course: Cretaceous* (pp. 1–283). Tipografia Pontefelcino, Perugia (Italy): Universities of Perugia and Milan.
- Rojay, B. (2013). Tectonic evolution of the Cretaceous Ankara Ophiolitic Mélange during the Late Cretaceous to pre-Miocene interval in central Anatolia, Turkey. *Journal of Geodynamics*, 65, 66–81. <https://doi.org/10.1016/j.jog.2012.06.006>
- Rojay, B., Altın, D., Özkan-Altın, S., Önen, A. P., James, S., & Thirlwall, M. F. (2004). Geodynamic significance of the Cretaceous pillow basalts from North Anatolian Ophiolitic Melange Belt (Central Anatolia, Turkey): Geochemical and paleontological constraints. *Geodinamica Acta*, 17(5), 349–361. <https://doi.org/10.3166/ga.17.349-361>
- Rojay, B., & Süzen, M. L. (1997). Tectonostratigraphic evolution of the Cretaceous dynamic basins on accretionary ophiolitic melange prism, SW of Ankara region. *Turkish Association of Petroleum Geologists Bulletin*, 9, 1–12.
- Rosenbaum, G., Lister, G. S., & Duboz, C. (2002). Relative motions of Africa, Iberia and Europe during alpine orogeny. *Tectonophysics*, 359(1–2), 117–129. [https://doi.org/10.1016/S0040-1951\(02\)00442-0](https://doi.org/10.1016/S0040-1951(02)00442-0)
- Sariaslan, N., & Altın, S. (2017). Planktonic foraminifera biostratigraphy of the Cenomanian–Campanian succession in the Haymana-Polatlı Basin (Ankara, Turkey). *Berichte der Geologischen Bundesanstalt*, 120, 235. Retrieved from https://opac.geologie.ac.at/www-opac/wwwopac.ashx?command=getcontent&server=images&value=BR0120_235.pdf
- Sarıfakıoğlu, E., Dilek, Y., & Sevin, M. (2014). Jurassic–Paleogene intraoceanic magmatic evolution of the Ankara Mélange, north-central Anatolia, Turkey. *Solid Earth*, 5(1), 77–108. <https://doi.org/10.5194/se-5-77-2014>
- Şengör, A. M. C., & Yılmaz, Y. (1981). Tethyan evolution of Turkey, a plate tectonic approach. *Tectonophysics*, 75(3–4), 181–241. [https://doi.org/10.1016/0040-1951\(81\)90275-4](https://doi.org/10.1016/0040-1951(81)90275-4)
- Şengör, A. M. C., Yılmaz, Y., & Ketin, İ. (1982). Remnants of a pre-late Jurassic Ocean in northern Turkey: Fragments of Permo-Triassic Paleo-Tethys? *Geological Society of America Bulletin*, 93, 932–936.
- Sharman, G. R., Graham, S. A., Grove, M., Kimbrough, D. L., & Wright, J. E. (2015). Detrital zircon provenance of the Late Cretaceous–Eocene California forearc: Influence of Laramide low-angle subduction on sediment dispersal and paleogeography. *Geological Society of America Bulletin*, 127(1–2), 38–60. <https://doi.org/10.1130/B31065.1>
- Speciale, P. A., Catlos, E. J., Yıldız, G. O., Shin, T. A., & Black, K. N. (2014). Zircon ages from the Beypazarı granitoid pluton (north central Turkey): Tectonic implications. *Geodinamica Acta*, 25, 162–182.
- Stern, R. J. (2002). Subduction zones. *Reviews of Geophysics*, 40(4), 1012. <https://doi.org/10.1029/2001RG000108>
- Stern, R. J. (2004). Subduction initiation: Spontaneous and induced. *Earth and Planetary Science Letters*, 226(3–4), 275–292. [https://doi.org/10.1016/S0012-821X\(04\)00498-4](https://doi.org/10.1016/S0012-821X(04)00498-4)
- Stern, R. J., & Gerya, T. (2018). Subduction initiation in nature and models: A review. *Tectonophysics*, 746, 173–198. <https://doi.org/10.1016/j.tecto.2017.10.014>
- Taira, A. (2001). Tectonic evolution of the Japanese island arc system. *Annual Review of Earth and Planetary Sciences*, 29(1), 109–134. <https://doi.org/10.1146/annurev.earth.29.1.109>
- Tankut, A., Dilek, Y., & Önen, P. (1998). Petrology and geochemistry of the Neo-Tethyan volcanism as revealed in the Ankara Melange Turkey. *Journal of Volcanology and Geothermal Research*, 85(1–4), 265–284. [https://doi.org/10.1016/S0377-0273\(98\)00059-6](https://doi.org/10.1016/S0377-0273(98)00059-6)
- Torelli, L., Sartorit, R., & Zitellini, N. (1997). The giant chaotic body in the Atlantic Ocean off Gibraltar: New results from a deep seismic reflection survey. *Marine and Petroleum Geology*, 14(2), 125–138. [https://doi.org/10.1016/S0264-8172\(96\)00060-8](https://doi.org/10.1016/S0264-8172(96)00060-8)
- Toth, J., & Gurnis, M. (1998). Dynamics of subduction initiation at preexisting fault zones. *Journal of Geophysical Research*, 103(B8), 18,053–18,067. <https://doi.org/10.1029/98JB01076>
- Tunç, M. (1993). Biostratigraphy of the pelagic limestones in the Aktaş (Kızılcahamam) region (in Turkish) *Proceedings of the A. Suat Erk Geology Symposium* (pp. 171–182). Ankara.
- Turhan, N. (2002). *Geological Map of Turkey, Ankara Sheet 1:500,000 Scale*. Ankara: Maden Tetkik ve Arama Genel Müdürlüğü.

- Ünalın, G. (1981). Stratigraphy of the “Ankara mélangé” southwest of Ankara (in Turkish). In *Proceedings of the Symposium on the Central Anatolian Geology* (pp. 46-52). Türkiye Jeoloji Kurumu, Ankara.
- Ünalın, G., Yüksel, V., Tekeli, T., Gönenç, O., Seyirt, Z., & Selahi, H. (1976). The Upper Cretaceous–Lower Tertiary stratigraphy and paleogeographic evolution of the Haymana-Polatlı region (southwest Ankara). *Türkiye Jeoloji Kurumu Bülteni*, *19*, 159–176.
- Üner, T., Çakır, Ü., Özdemir, Y., & Arat, İ. (2014). Geochemistry and origin of plagiogranites from the Eldivan ophiolite, Çankırı (central Anatolia, Turkey). *Geologica Carpathica*, *65*, 195–205.
- Uysal, I., Ersoy, E. Y., Dilek, Y., Kapsiotis, A., & Sarıfakıoğlu, E. (2016). Multiple episodes of partial melting, depletion, metasomatism and enrichment processes recorded in the heterogeneous upper mantle sequence of the Neotethyan Eldivan ophiolite, Turkey. *Lithos*, *246–247*, 228–245.
- Varol, B., & Gökten, E. (1994). The facies properties and depositional environments of nodular limestones and red marly limestones (Ammonitico Rosso) in the Ankara Jurassic sequence, central Turkey. *Terra Nova*, *6*(1), 64–71. <https://doi.org/10.1111/j.1365-3121.1994.tb00634.x>
- Varol, E., Temel, A., Yürür, T., Gourgaud, A., & Bello, H. (2014). Petrogenesis of the Neogene bimodal magmatism of the Galatean Volcanic Province, central Anatolia, Turkey. *Journal of Volcanology and Geothermal Research*, *280*, 14–29. <https://doi.org/10.1016/j.jvolgeores.2014.04.014>
- Vincent, S. J., Guo, L., Flecker, R., BouDagher-Fadel, M. K., Ellam, R. M., & Kandemir, R. (2018). Age constraints on intra-formational unconformities in Upper Jurassic–Lower Cretaceous carbonates in northeast Turkey; geodynamic and hydrocarbon implications. *Marine and Petroleum Geology*, *91*, 639–657. <https://doi.org/10.1016/j.marpetgeo.2018.01.011>
- Vörös, A. (2014). A taxonomic and nomenclatural revision of the historical brachiopod collection from the Lower Jurassic of Yakacık (Ankara, Turkey), housed in the Geological and Geophysical Institute of Hungary. *Földtani Közlemények*, *144*, 231–254.
- Whitney, D. L., & Hamilton, M. A. (2004). Timing of high-grade metamorphism in central Turkey and the assembly of Anatolia. *Journal of Geological Society*, *161*(5), 823–828. <https://doi.org/10.1144/0016-764903-081>
- Yılmaz, İ. Ö. (2008). Cretaceous pelagic red beds and black shales (Aptian–Santonian), NW Turkey: Global oceanic anoxic and oxic events. *Turkish Journal of Earth Sciences*, *17*, 263–296.